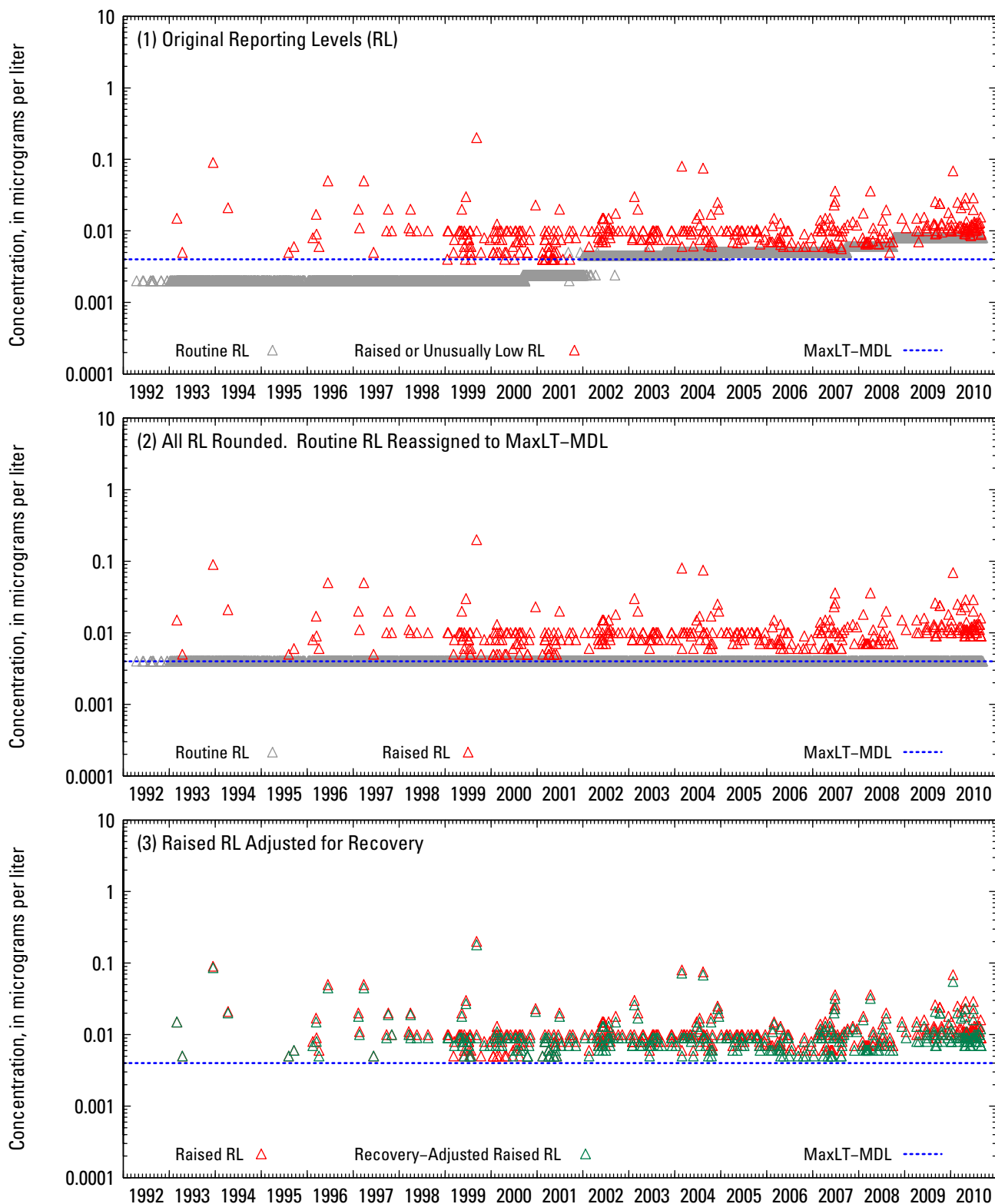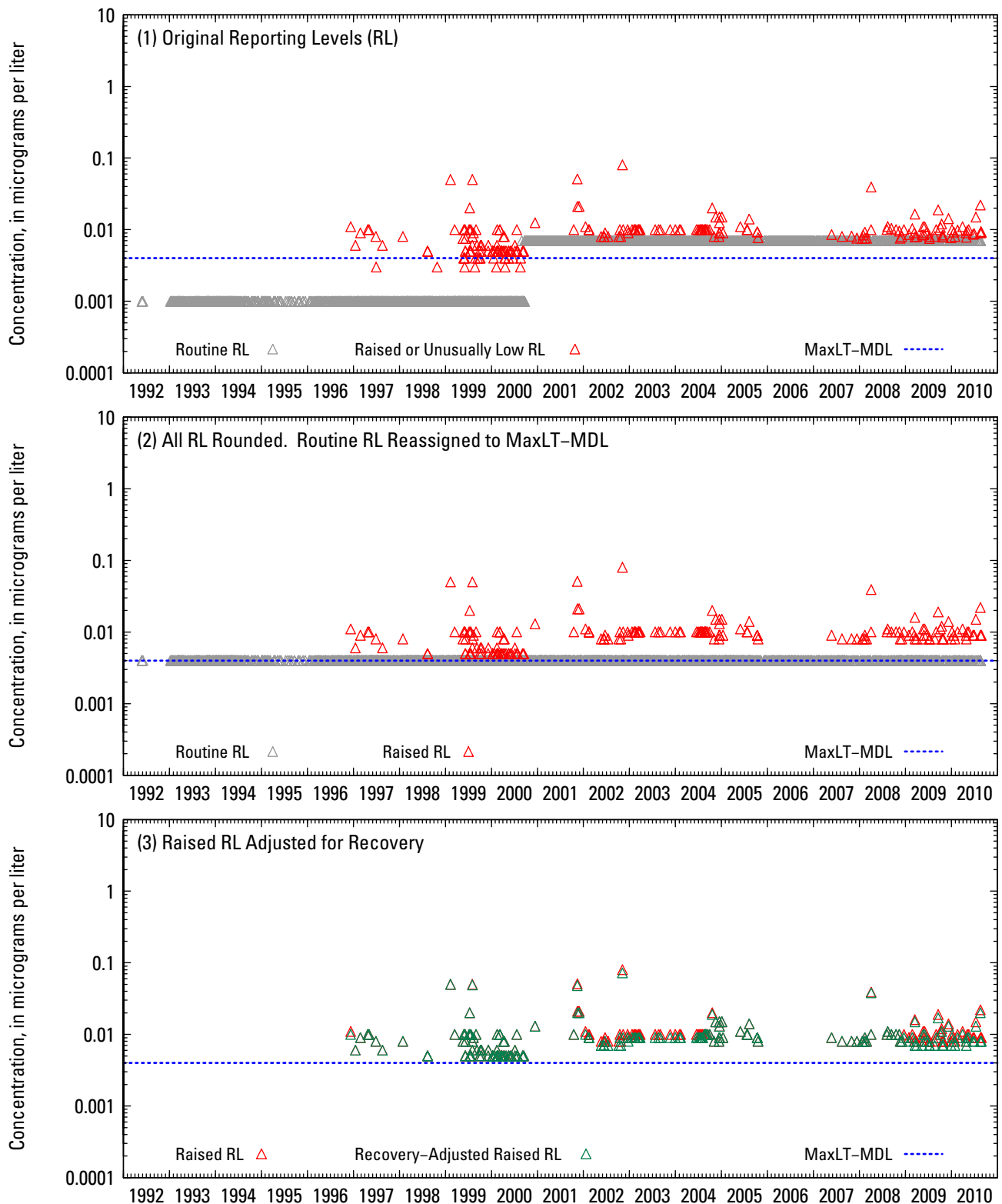**Figure 1–1.** Time–series plots of nondetections of acetochlor for all sites in the trend dataset showing (1) original reporting levels; (2) rounded reporting levels and, for routine nondetections, reporting levels reassigned to the maximum value of the long–term method detection level (maxLT–MDL); and (3) raised reporting levels adjusted for temporal changes in recovery. Temporal changes in recovery are shown in panel 2 of the figures in appendix 2.
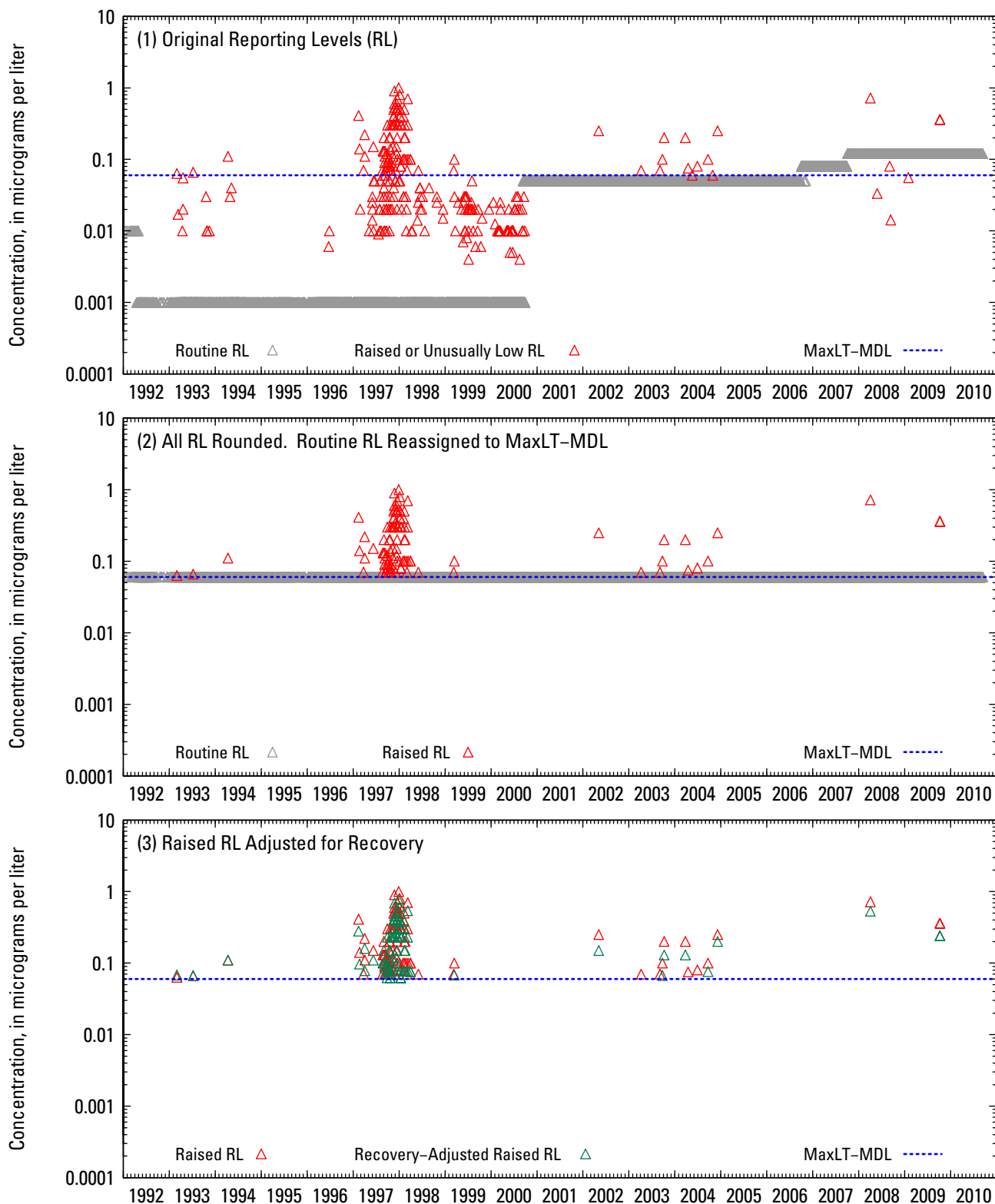
Figure 1–2. Time–series plots of nondetections of alachlor for all sites in the trend dataset showing (1) original reporting levels; (2) rounded reporting levels and, for routine nondetections, reporting levels reassigned to the maximum value of the long–term method detection level (maxLT–MDL); and (3) raised reporting levels adjusted for temporal changes in recovery. Temporal changes in recovery are shown in panel 2 of the figures in appendix 2.
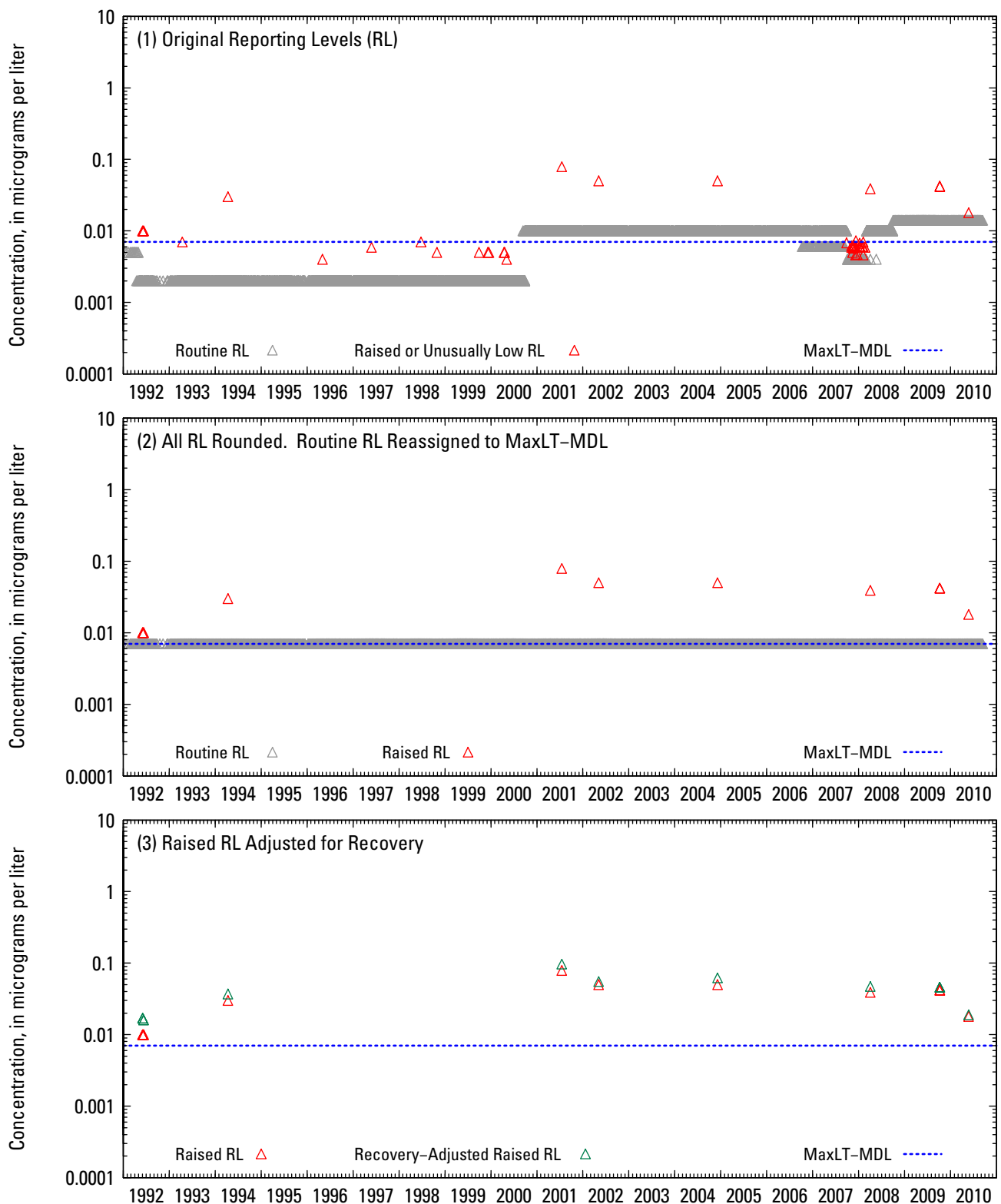
Figure 1–3. Time–series plots of nondetections of atrazine for all sites in the trend dataset showing (1) original reporting levels; (2) rounded reporting levels and, for routine nondetections, reporting levels reassigned to the maximum value of the long–term method detection level (maxLT–MDL); and (3) raised reporting levels adjusted for temporal changes in recovery. Temporal changes in recovery are shown in panel 2 of the figures in appendix 2.
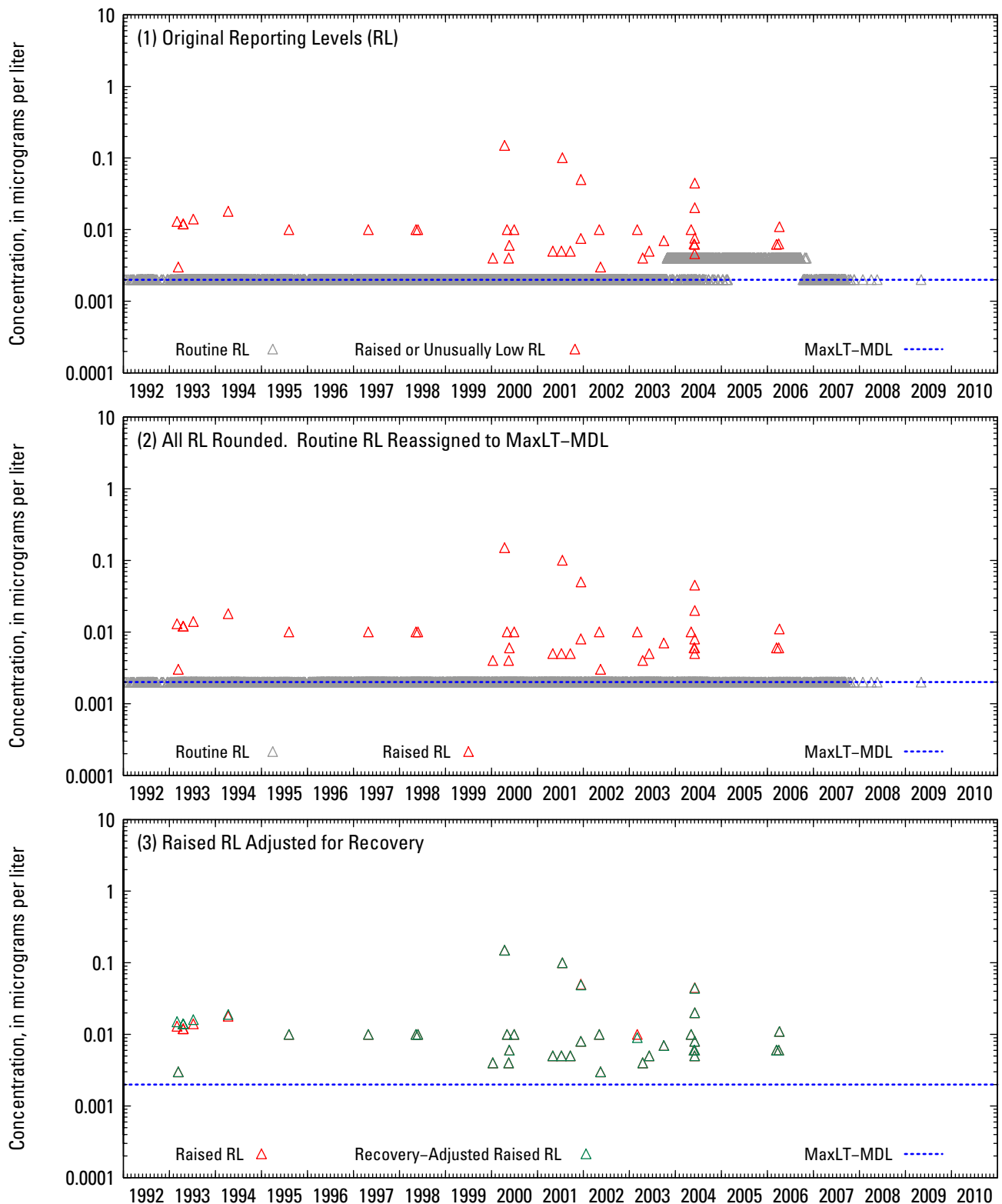
Figure 1–4. Time–series plots of nondetections of azinphos–methyl for all sites in the trend dataset showing (1) original reporting levels; (2) rounded reporting levels and, for routine nondetections, reporting levels reassigned to the maximum value of the long–term method detection level (maxLT–MDL); and (3) raised reporting levels adjusted for temporal changes in recovery. Temporal changes in recovery are shown in panel 2 of the figures in appendix 2.
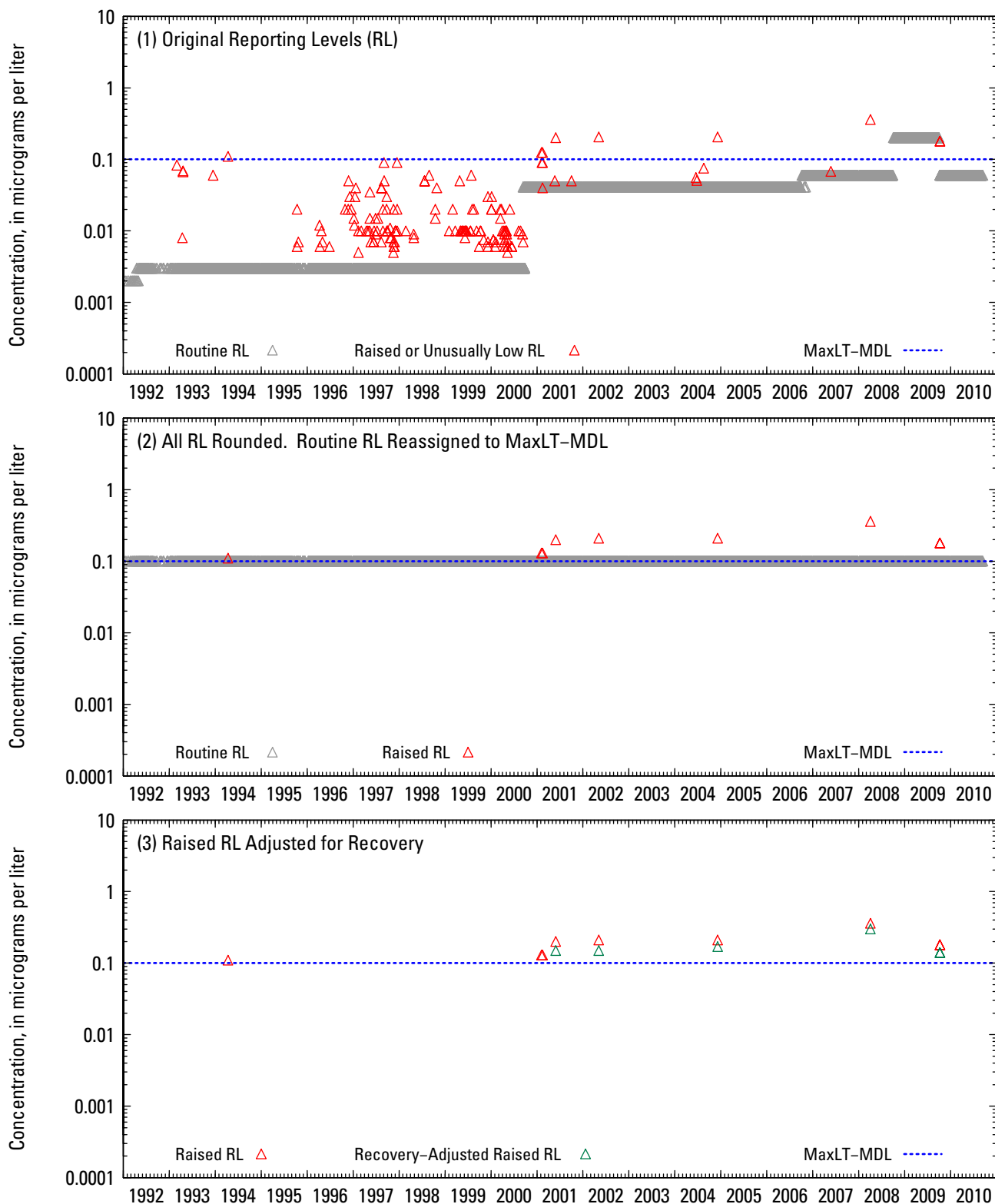
Figure 1–5. Time–series plots of nondetections of benfluralin for all sites in the trend dataset showing (1) original reporting levels; (2) rounded reporting levels and, for routine nondetections, reporting levels reassigned to the maximum value of the long–term method detection level (maxLT–MDL); and (3) raised reporting levels adjusted for temporal changes in recovery. Temporal changes in recovery are shown in panel 2 of the figures in appendix 2.
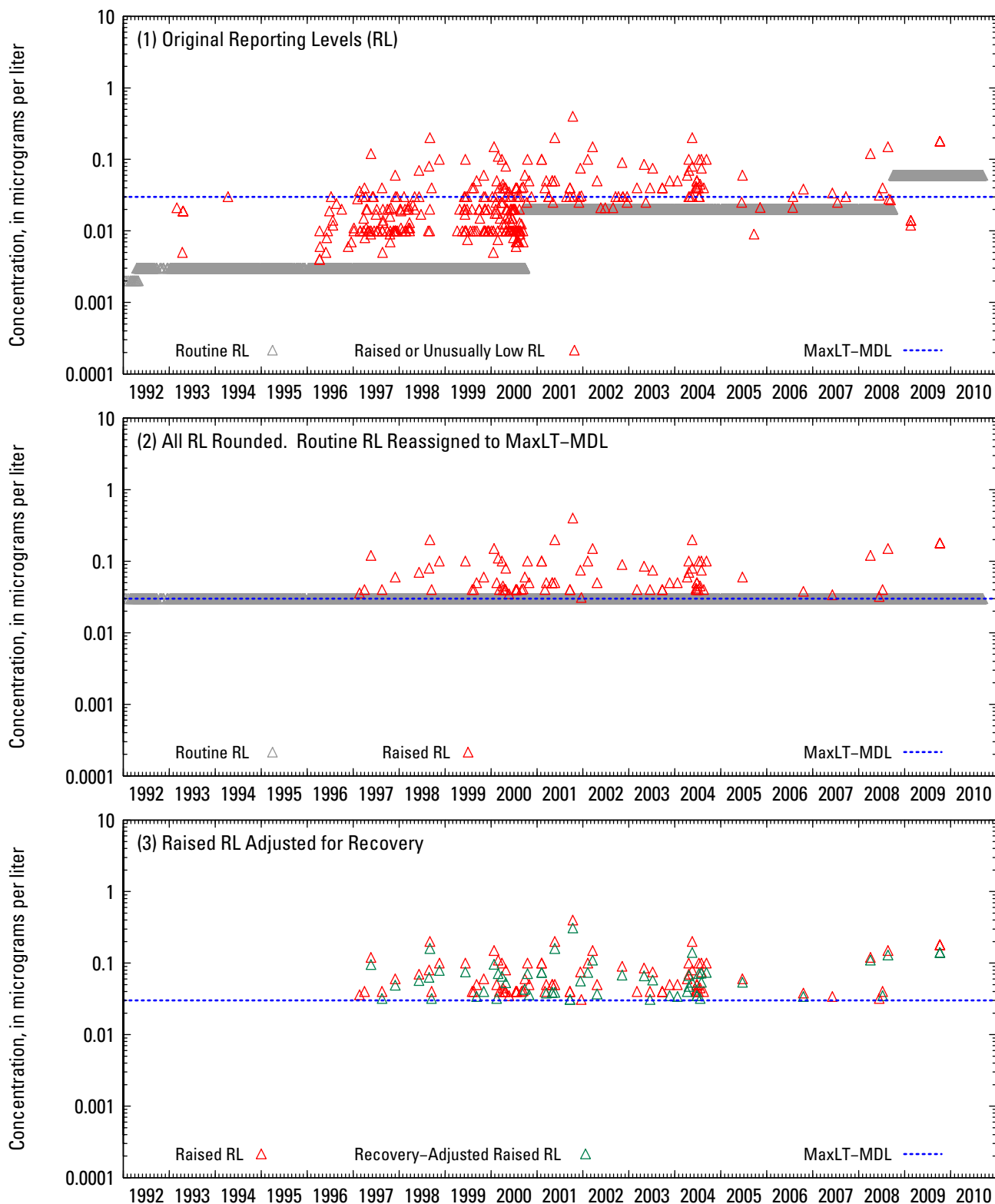
Figure 1–6. Time–series plots of nondetections of butylate for all sites in the trend dataset showing (1) original reporting levels; (2) rounded reporting levels and, for routine nondetections, reporting levels reassigned to the maximum value of the long–term method detection level (maxLT–MDL); and (3) raised reporting levels adjusted for temporal changes in recovery. Temporal changes in recovery are shown in panel 2 of the figures in appendix 2.

Figure 1–7. Time–series plots of nondetections of carbaryl for all sites in the trend dataset showing (1) original reporting levels; (2) rounded reporting levels and, for routine nondetections, reporting levels reassigned to the maximum value of the long–term method detection level (maxLT–MDL); and (3) raised reporting levels adjusted for temporal changes in recovery. Temporal changes in recovery are shown in panel 2 of the figures in appendix 2.
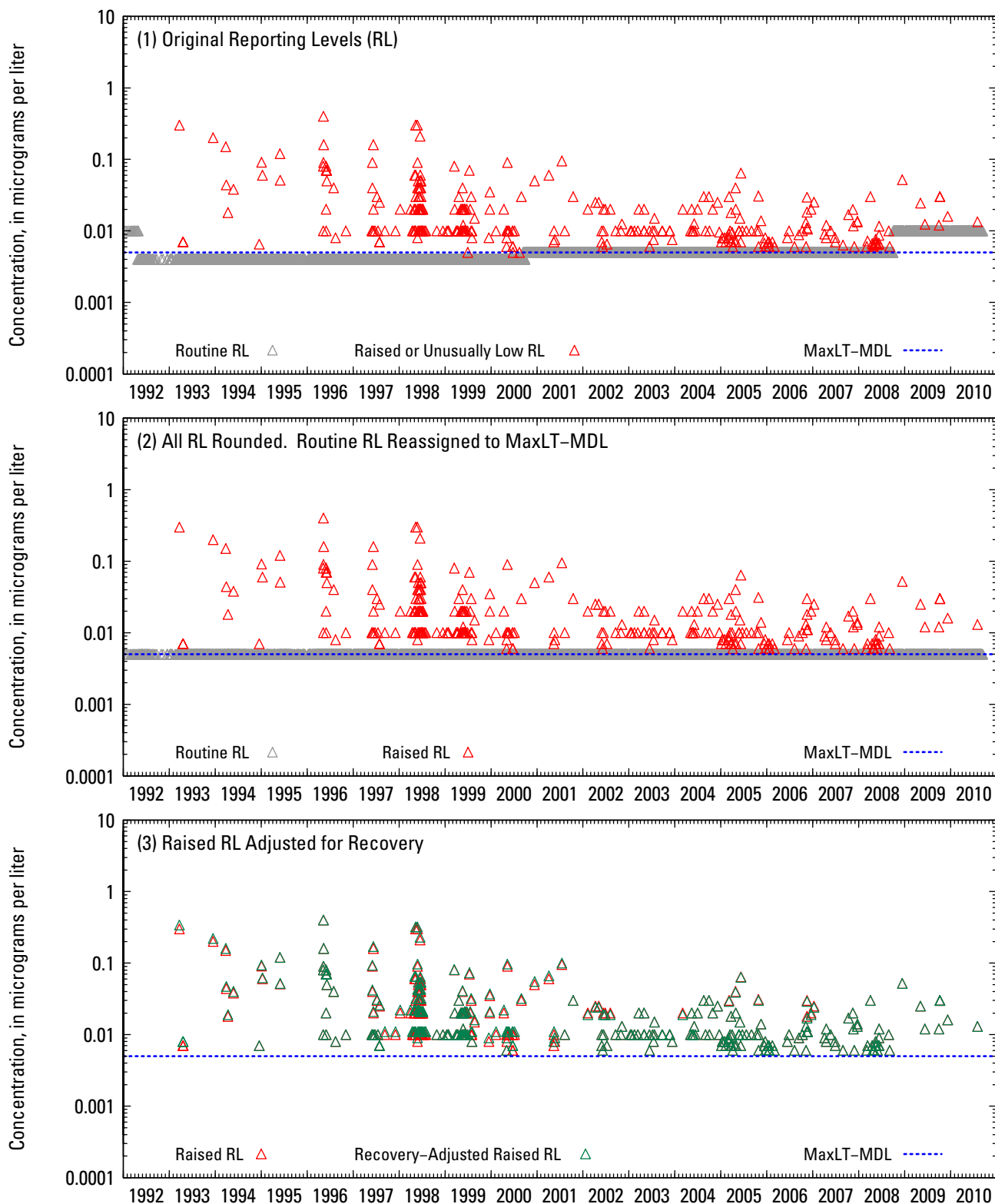
Figure 1–8. Time–series plots of nondetections of carbofuran for all sites in the trend dataset showing (1) original reporting levels; (2) rounded reporting levels and, for routine nondetections, reporting levels reassigned to the maximum value of the long–term method detection level (maxLT–MDL); and (3) raised reporting levels adjusted for temporal changes in recovery. Temporal changes in recovery are shown in panel 2 of the figures in appendix 2.
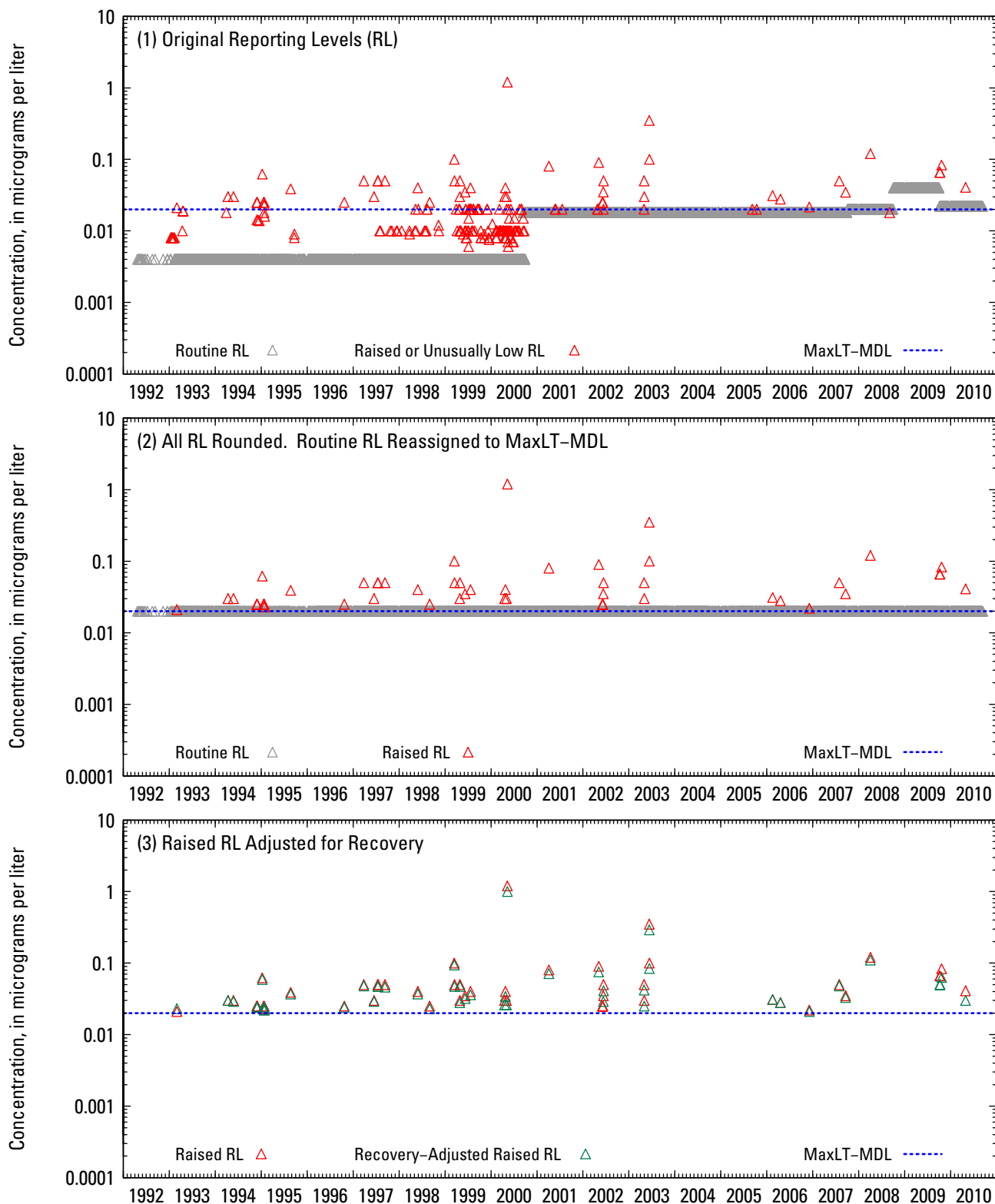
Figure 1–9. Time–series plots of nondetections of chlorpyrifos for all sites in the trend dataset showing (1) original reporting levels; (2) rounded reporting levels and, for routine nondetections, reporting levels reassigned to the maximum value of the long–term method detection level (maxLT–MDL); and (3) raised reporting levels adjusted for temporal changes in recovery. Temporal changes in recovery are shown in panel 2 of the figures in appendix 2.
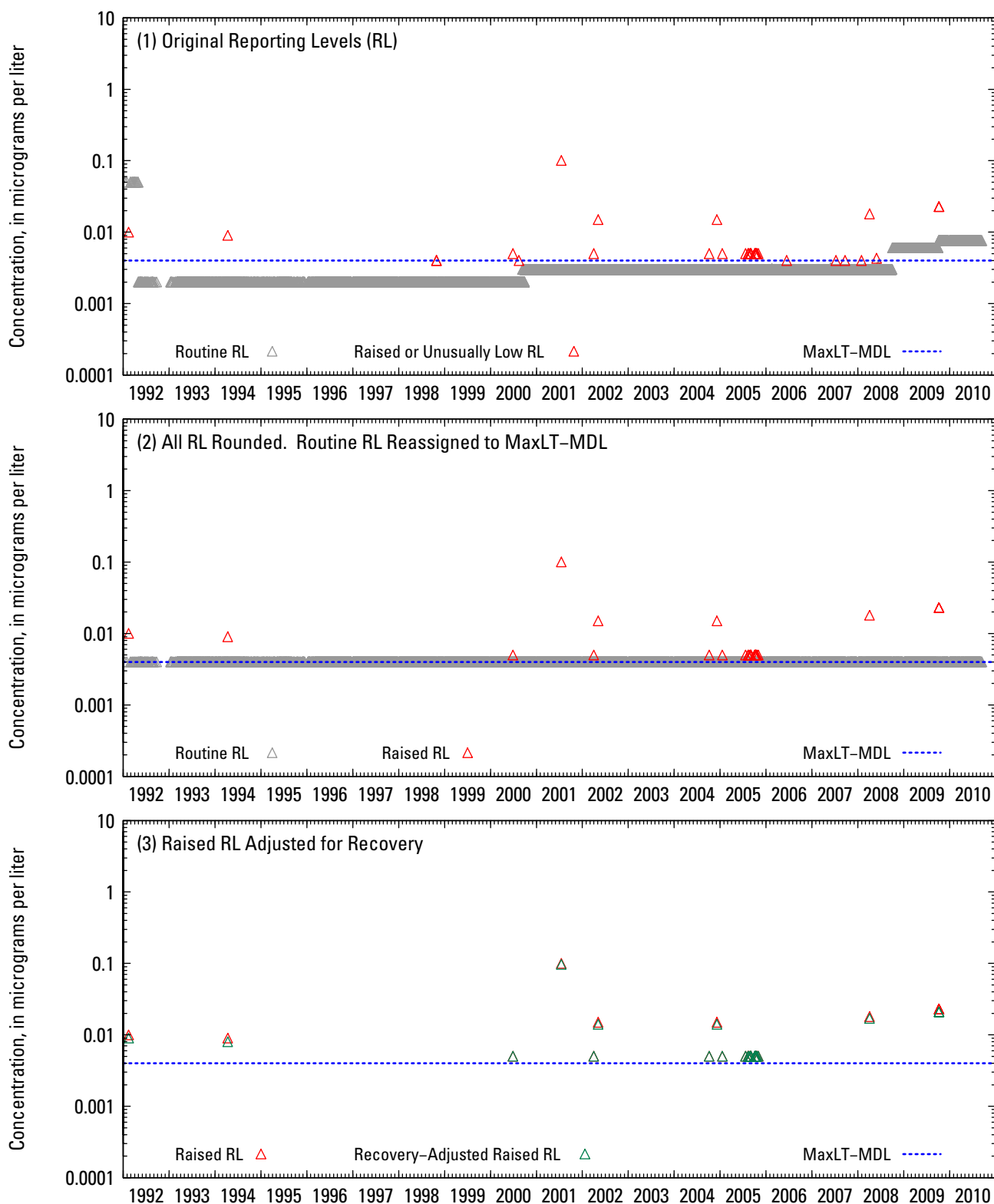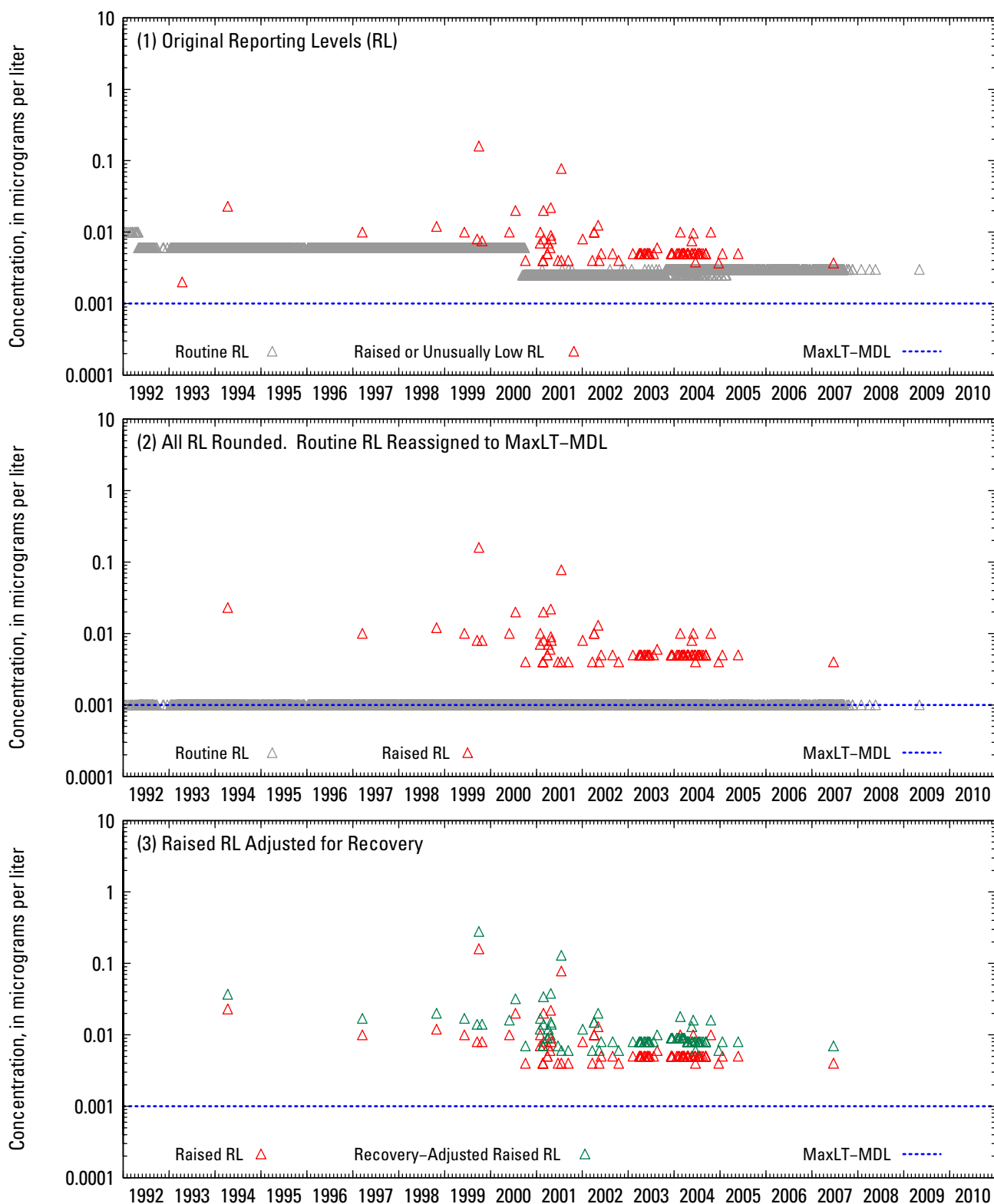
Figure 1–10. Time–series plots of nondetections of cyanazine for all sites in the trend dataset showing (1) original reporting levels; (2) rounded reporting levels and, for routine nondetections, reporting levels reassigned to the maximum value of the long–term method detection level (maxLT–MDL); and (3) raised reporting levels adjusted for temporal changes in recovery. Temporal changes in recovery are shown in panel 2 of the figures in appendix 2.
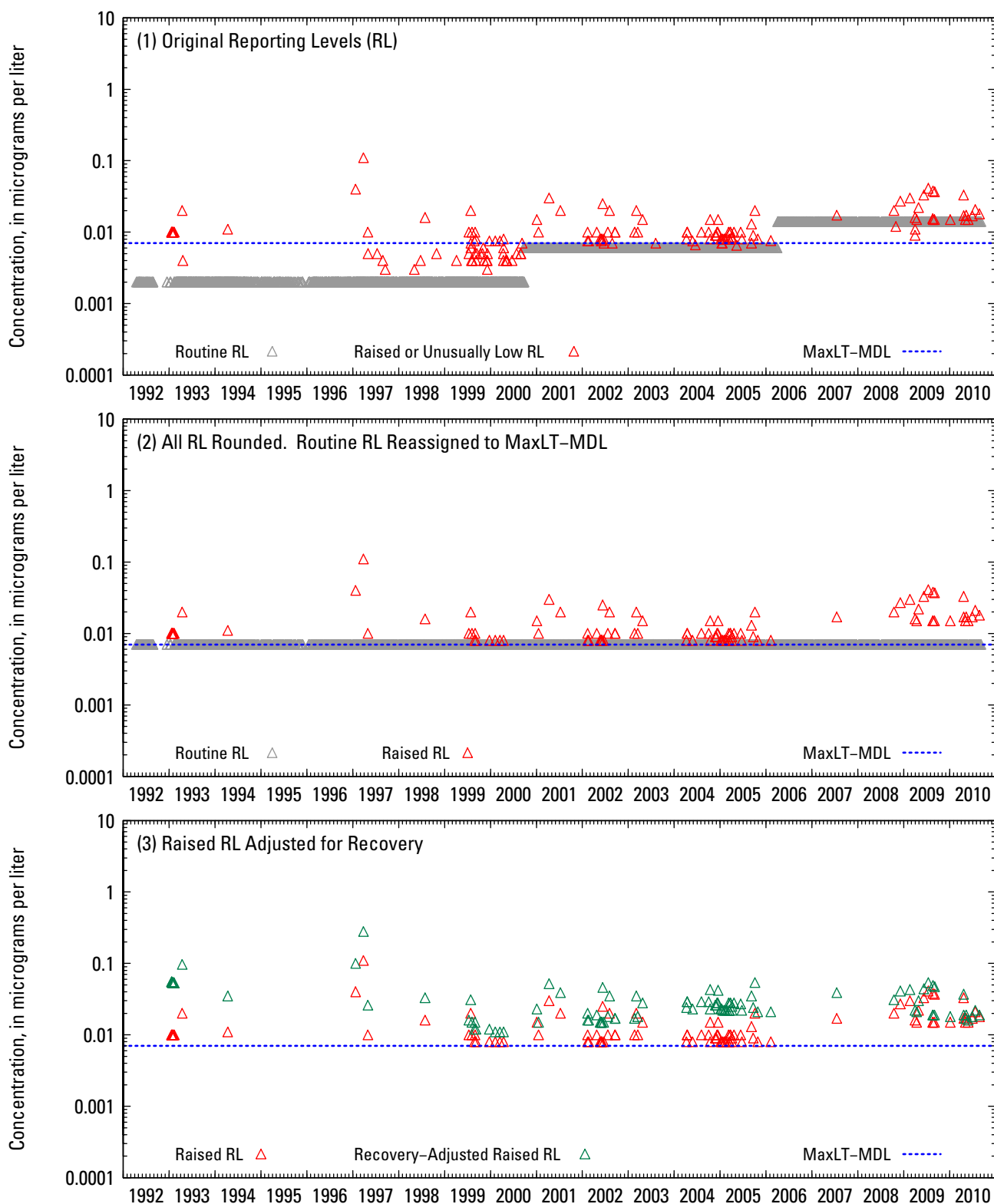
Figure 1–11. Time–series plots of nondetections of Dacthal® for all sites in the trend dataset showing (1) original reporting levels; (2) rounded reporting levels and, for routine nondetections, reporting levels reassigned to the maximum value of the long–term method detection level (maxLT–MDL); and (3) raised reporting levels adjusted for temporal changes in recovery. Temporal changes in recovery are shown in panel 2 of the figures in appendix 2.
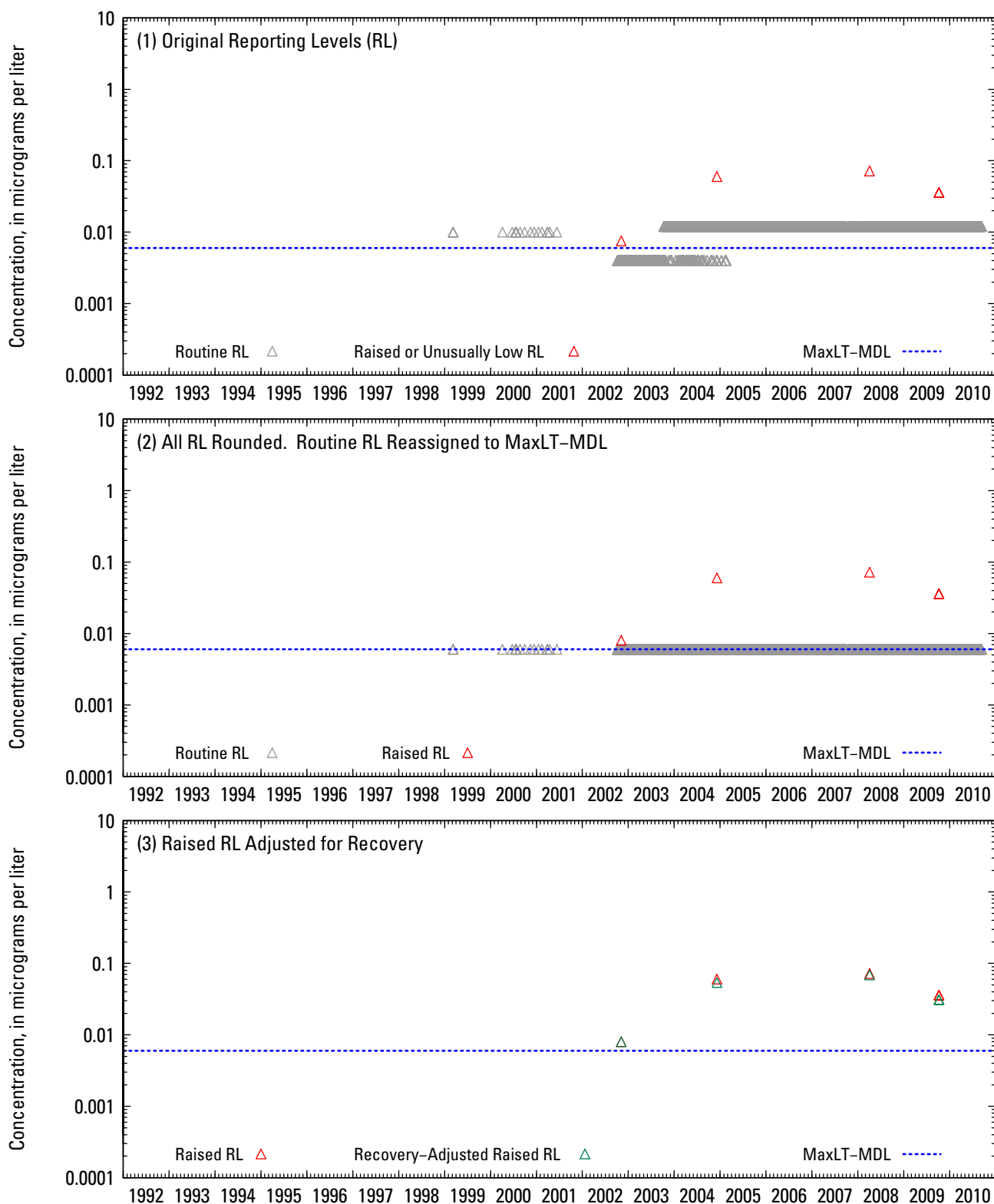
Figure 1–12. Time–series plots of nondetections of p,p'–DDE for all sites in the trend dataset showing (1) original reporting levels; (2) rounded reporting levels and, for routine nondetections, reporting levels reassigned to the maximum value of the long–term method detection level (maxLT–MDL); and (3) raised reporting levels adjusted for temporal changes in recovery. Temporal changes in recovery are shown in panel 2 of the figures in appendix 2.
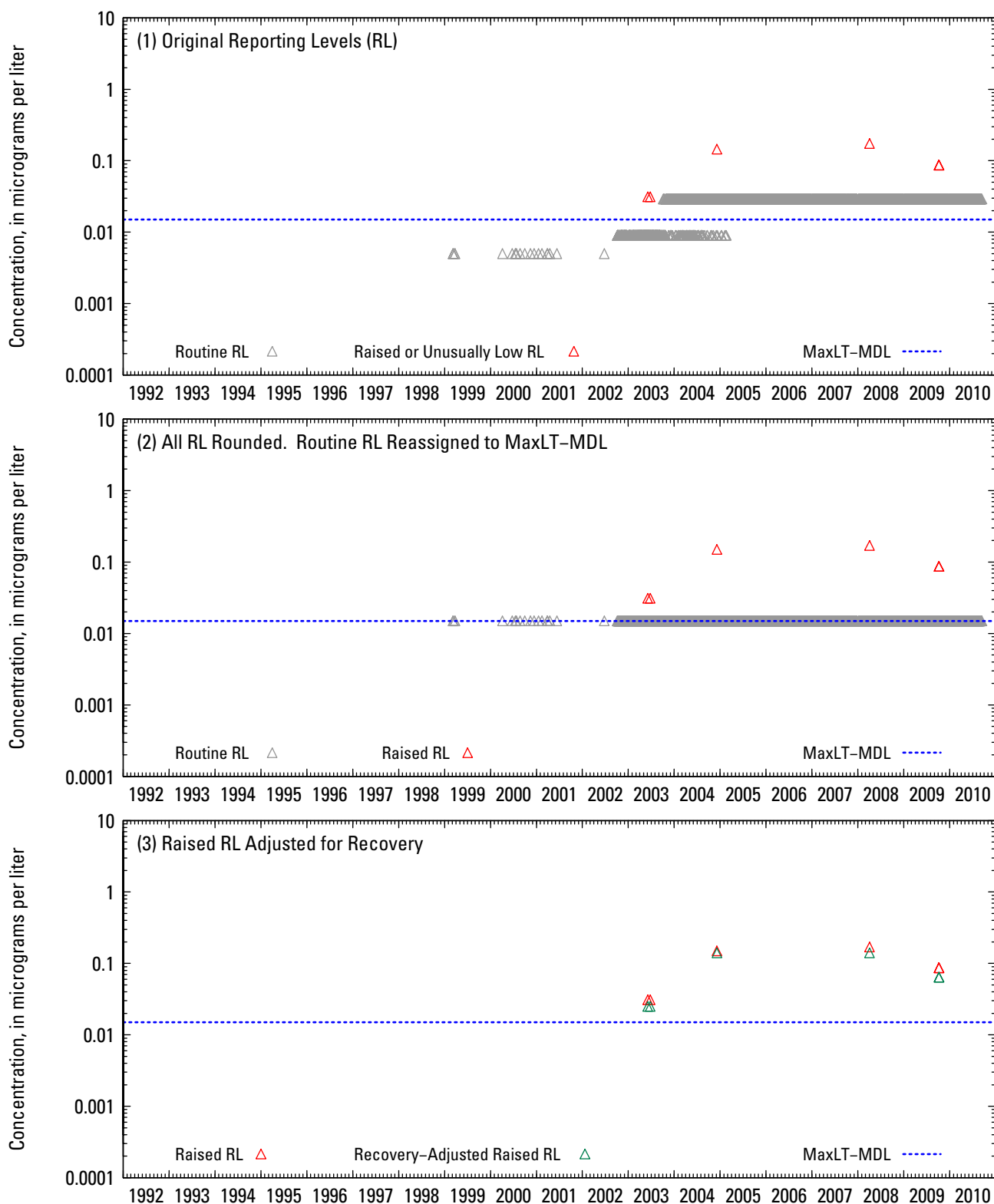
Figure 1–13. Time–series plots of nondetections of deethylatrazine for all sites in the trend dataset showing (1) original reporting levels; (2) rounded reporting levels and, for routine nondetections, reporting levels reassigned to the maximum value of the long–term method detection level (maxLT–MDL); and (3) raised reporting levels adjusted for temporal changes in recovery. Temporal changes in recovery are shown in panel 2 of the figures in appendix 2.
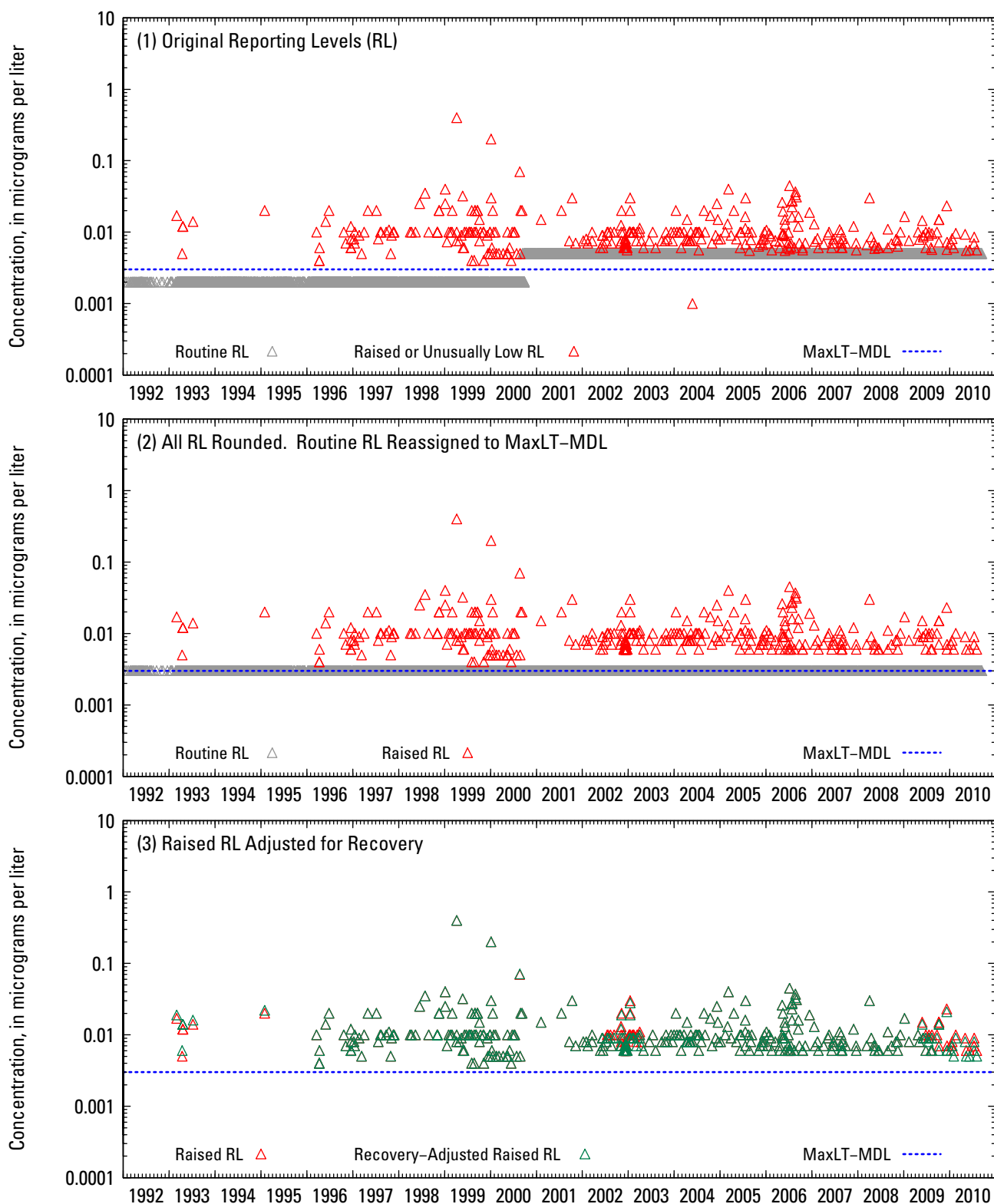
Figure 1–14. Time–series plots of nondetections of desulfinylfipronil for all sites in the trend dataset showing (1) original reporting levels; (2) rounded reporting levels and, for routine nondetections, reporting levels reassigned to the maximum value of the long–term method detection level (maxLT–MDL); and (3) raised reporting levels adjusted for temporal changes in recovery. Temporal changes in recovery are shown in panel 2 of the figures in appendix 2.

Figure 1–15. Time–series plots of nondetections of desulfinylfipronil amide for all sites in the trend dataset showing (1) original reporting levels; (2) rounded reporting levels and, for routine nondetections, reporting levels reassigned to the maximum value of the long–term method detection level (maxLT–MDL); and (3) raised reporting levels adjusted for temporal changes in recovery. Temporal changes in recovery are shown in panel 2 of the figures in appendix 2.
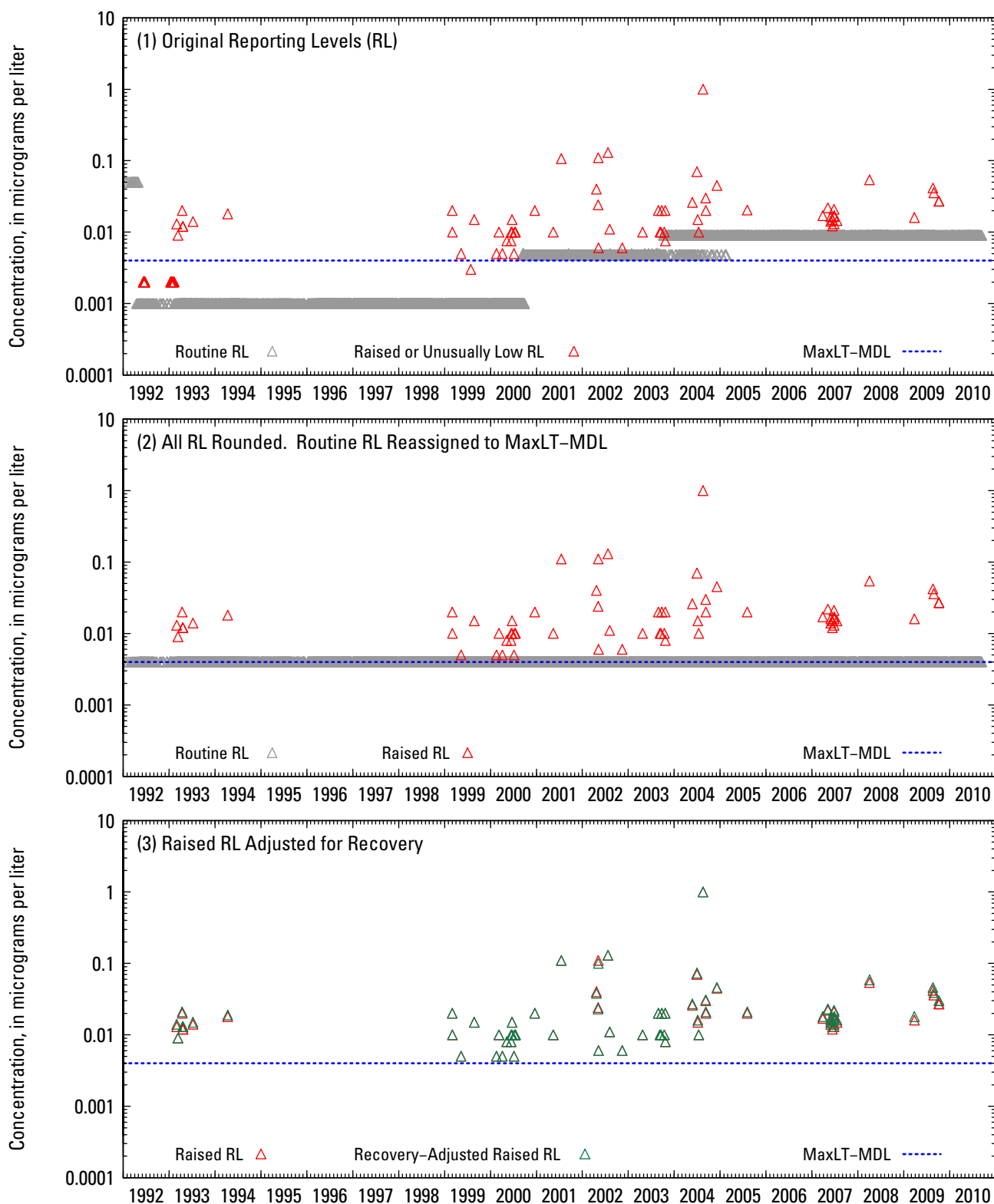
Figure 1–16. Time–series plots of nondetections of diazinon for all sites in the trend dataset showing (1) original reporting levels; (2) rounded reporting levels and, for routine nondetections, reporting levels reassigned to the maximum value of the long–term method detection level (maxLT–MDL); and (3) raised reporting levels adjusted for temporal changes in recovery. Temporal changes in recovery are shown in panel 2 of the figures in appendix 2.
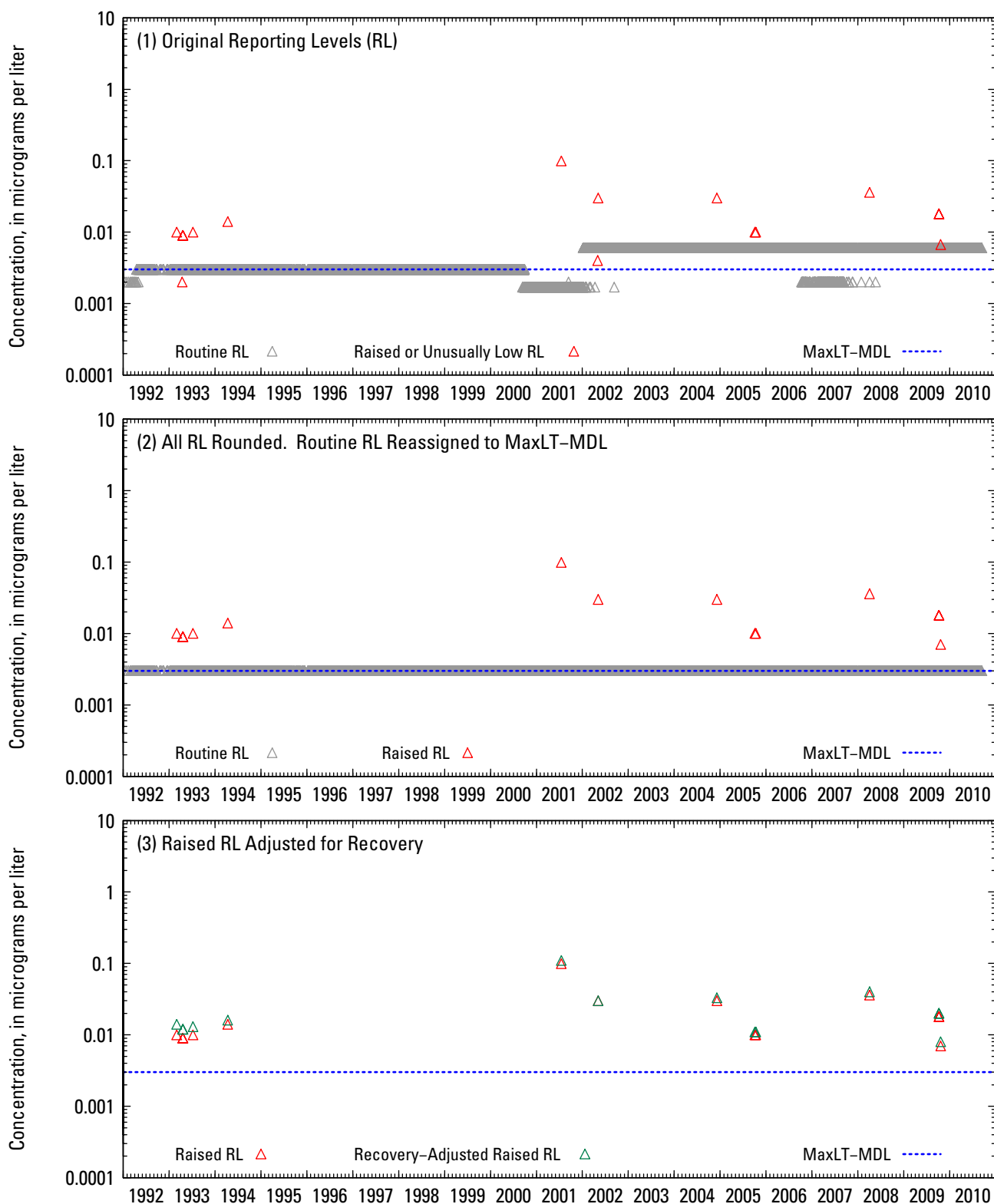
Figure 1–17. Time–series plots of nondetections of dieldrin for all sites in the trend dataset showing (1) original reporting levels; (2) rounded reporting levels and, for routine nondetections, reporting levels reassigned to the maximum value of the long–term method detection level (maxLT–MDL); and (3) raised reporting levels adjusted for temporal changes in recovery. Temporal changes in recovery are shown in panel 2 of the figures in appendix 2.
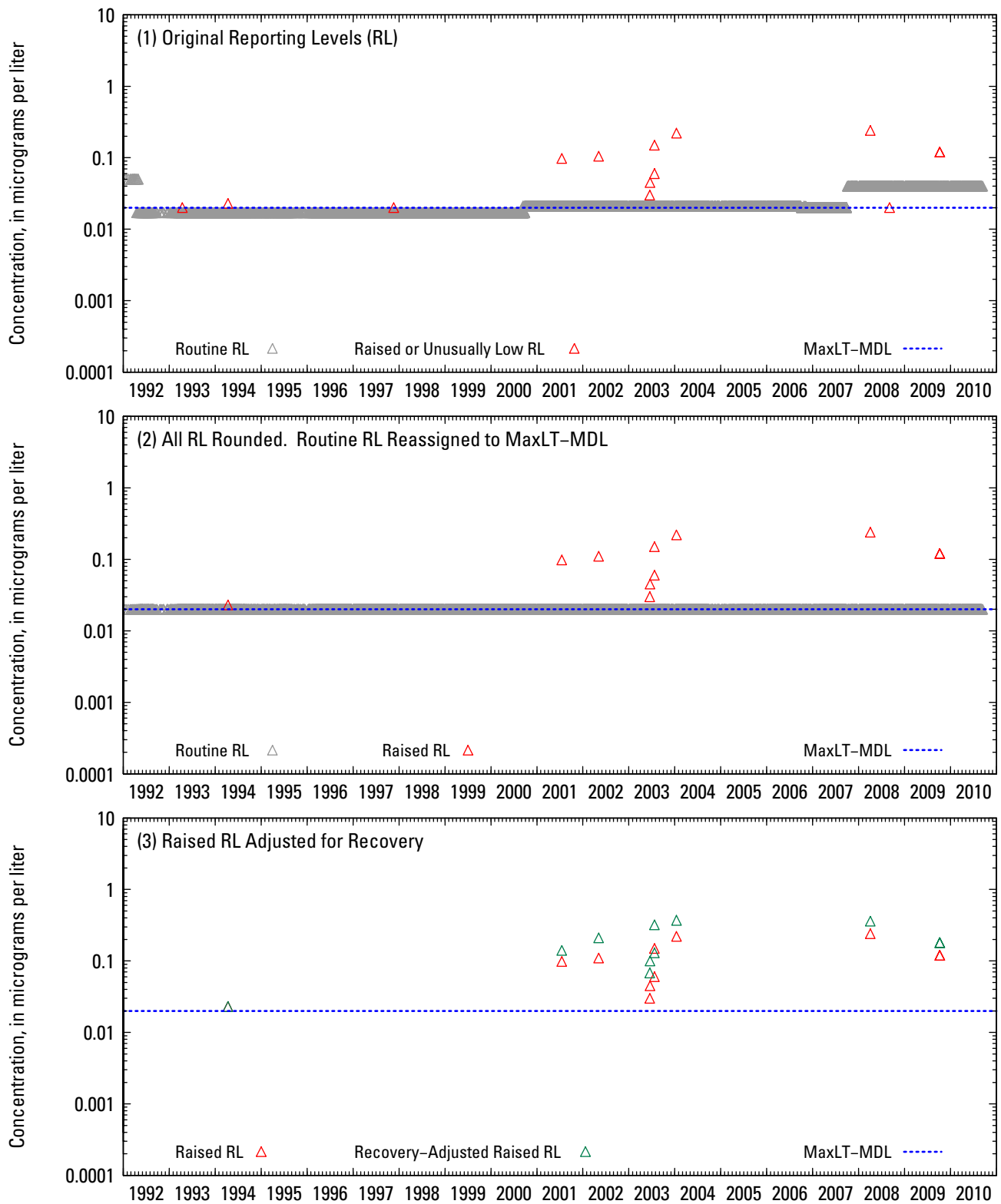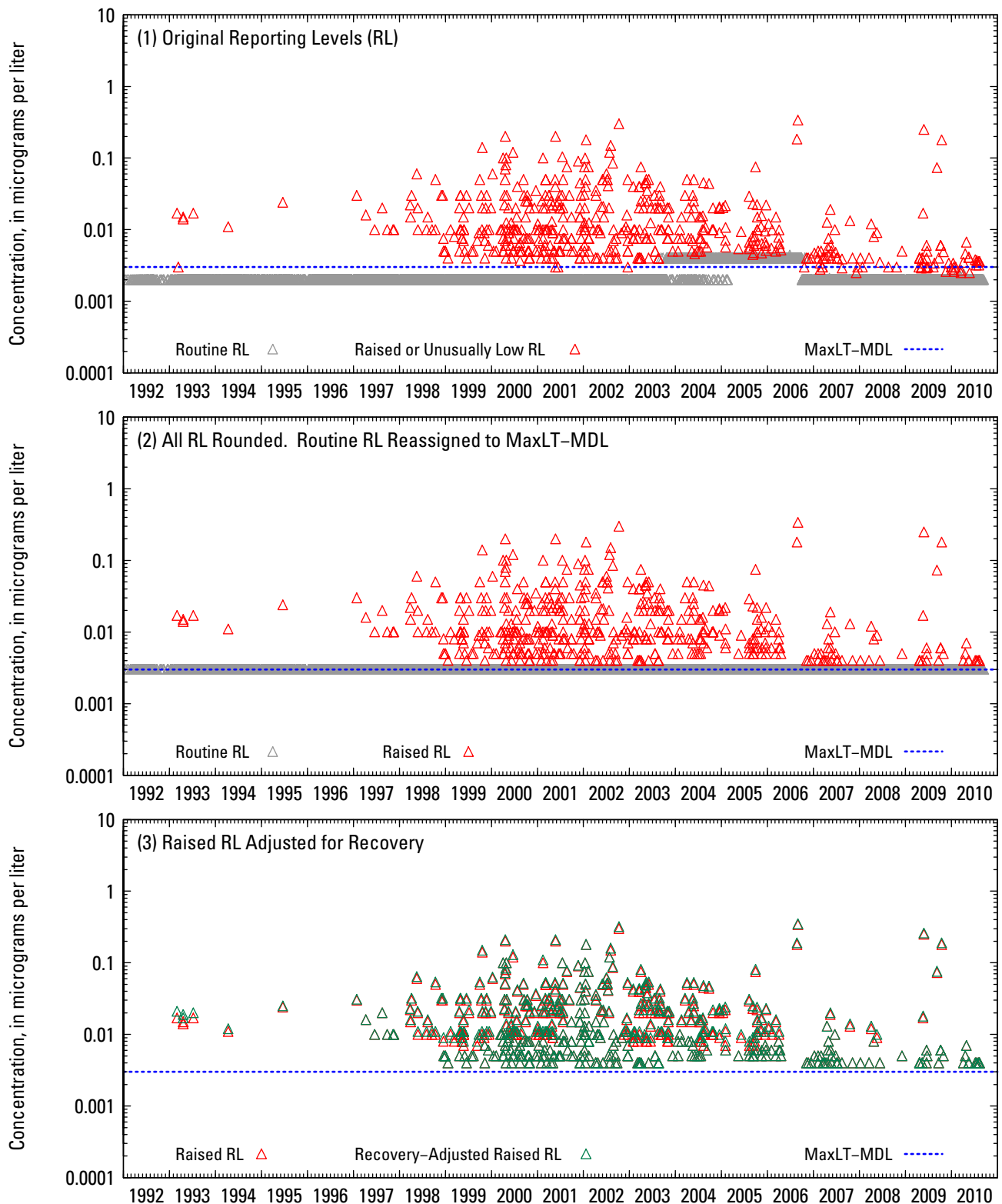
Figure 1–18. Time–series plots of nondetections of 2,6–diethylaniline for all sites in the trend dataset showing (1) original reporting levels; (2) rounded reporting levels and, for routine nondetections, reporting levels reassigned to the maximum value of the long–term method detection level (maxLT–MDL); and (3) raised reporting levels adjusted for temporal changes in recovery. Temporal changes in recovery are shown in panel 2 of the figures in appendix 2.
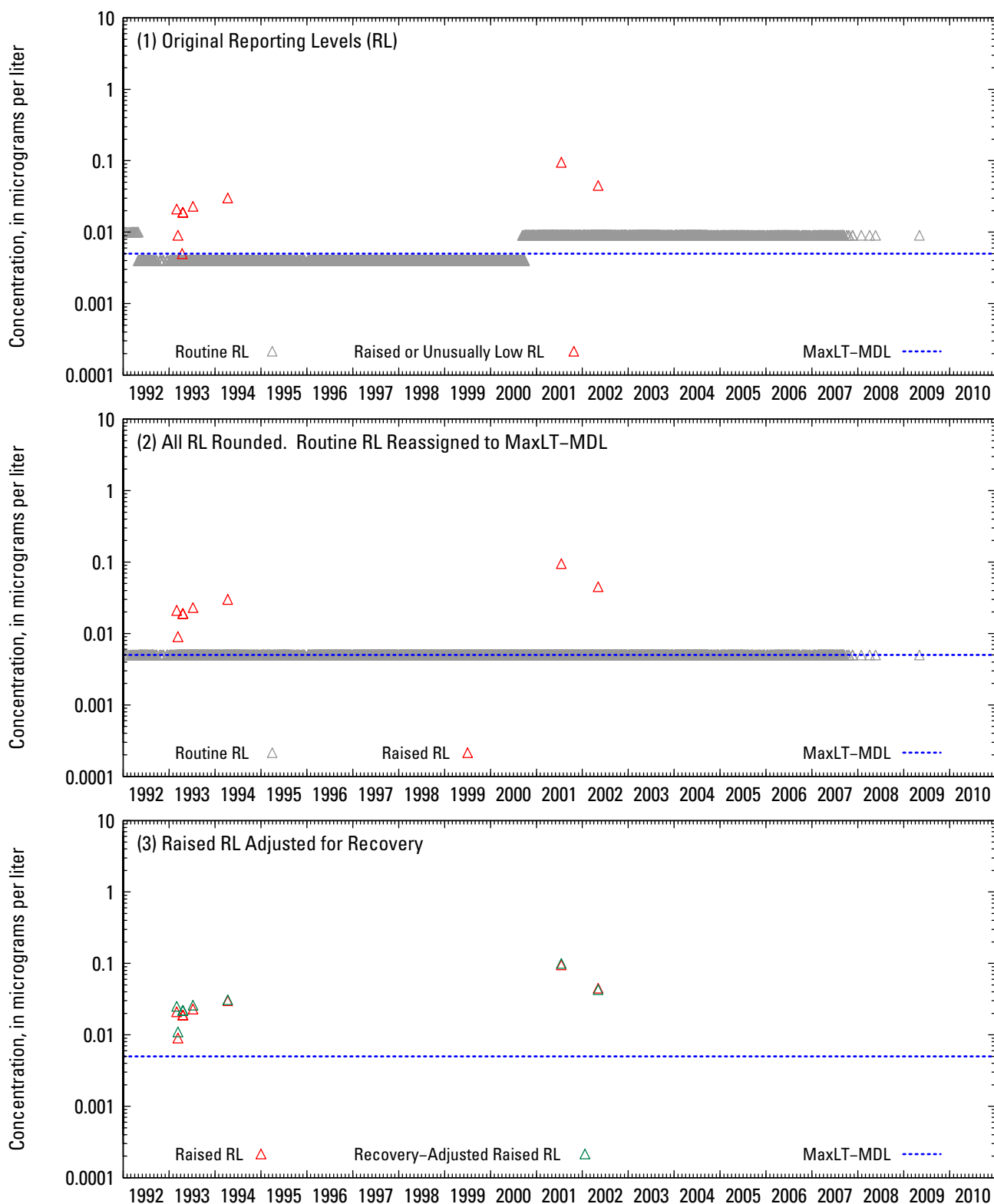
Figure 1–19. Time–series plots of nondetections of disulfoton for all sites in the trend dataset showing (1) original reporting levels; (2) rounded reporting levels and, for routine nondetections, reporting levels reassigned to the maximum value of the long–term method detection level (maxLT–MDL); and (3) raised reporting levels adjusted for temporal changes in recovery. Temporal changes in recovery are shown in panel 2 of the figures in appendix 2.
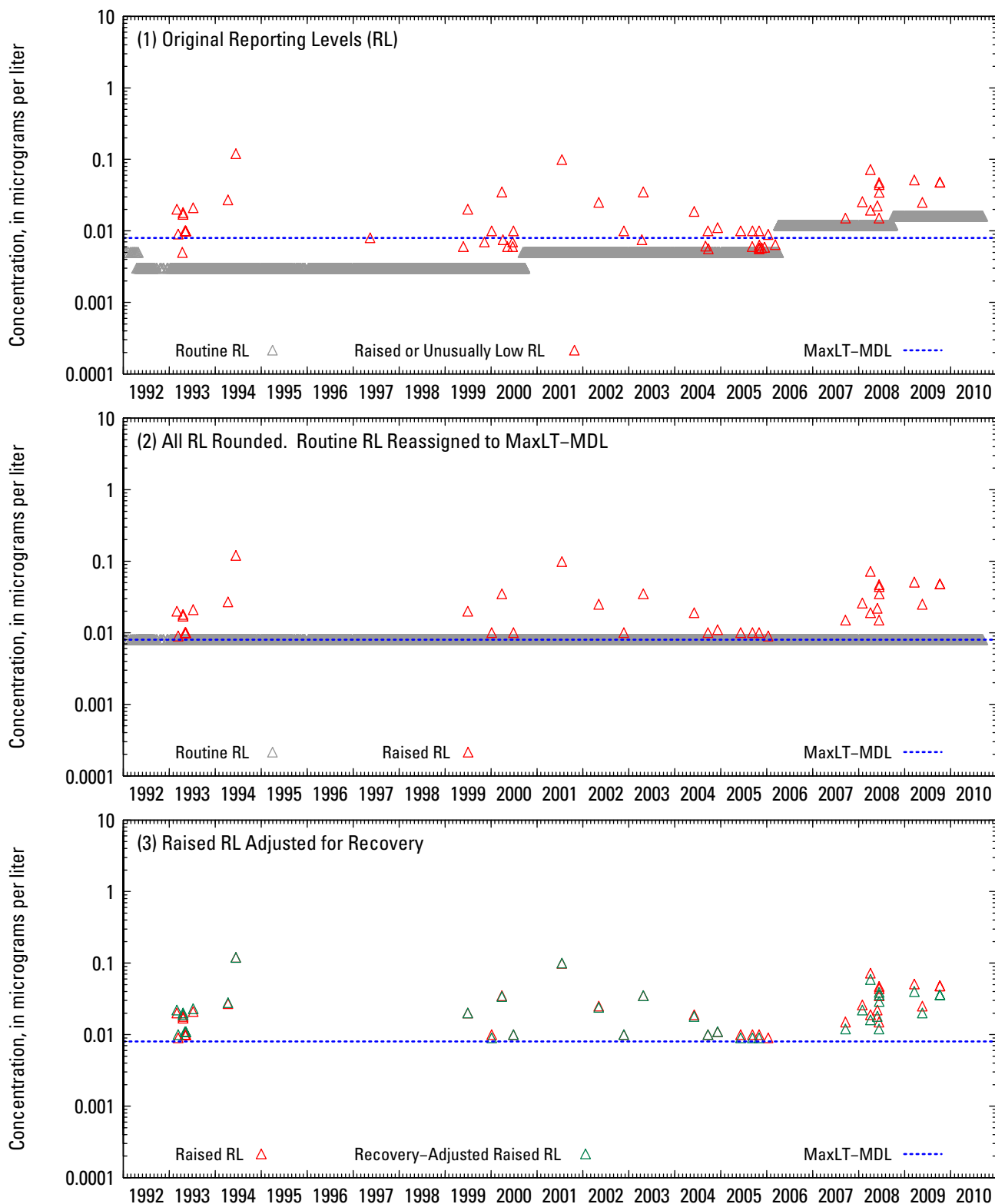
Figure 1–20. Time–series plots of nondetections of EPTC for all sites in the trend dataset showing (1) original reporting levels; (2) rounded reporting levels and, for routine nondetections, reporting levels reassigned to the maximum value of the long–term method detection level (maxLT–MDL); and (3) raised reporting levels adjusted for temporal changes in recovery. Temporal changes in recovery are shown in panel 2 of the figures in appendix 2.
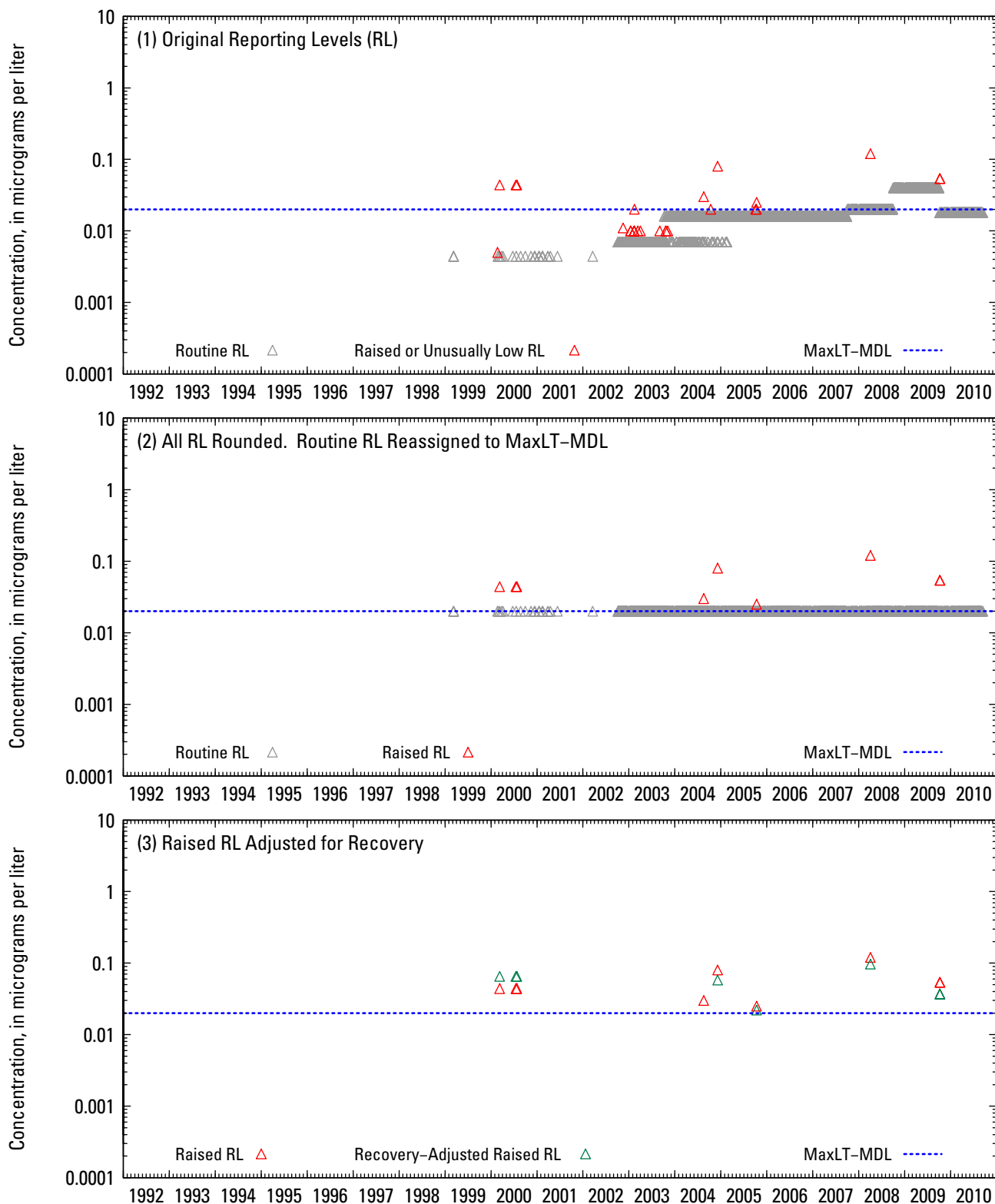
Figure 1–21. Time–series plots of nondetections of ethalfluralin for all sites in the trend dataset showing (1) original reporting levels; (2) rounded reporting levels and, for routine nondetections, reporting levels reassigned to the maximum value of the long–term method detection level (maxLT–MDL); and (3) raised reporting levels adjusted for temporal changes in recovery. Temporal changes in recovery are shown in panel 2 of the figures in appendix 2.
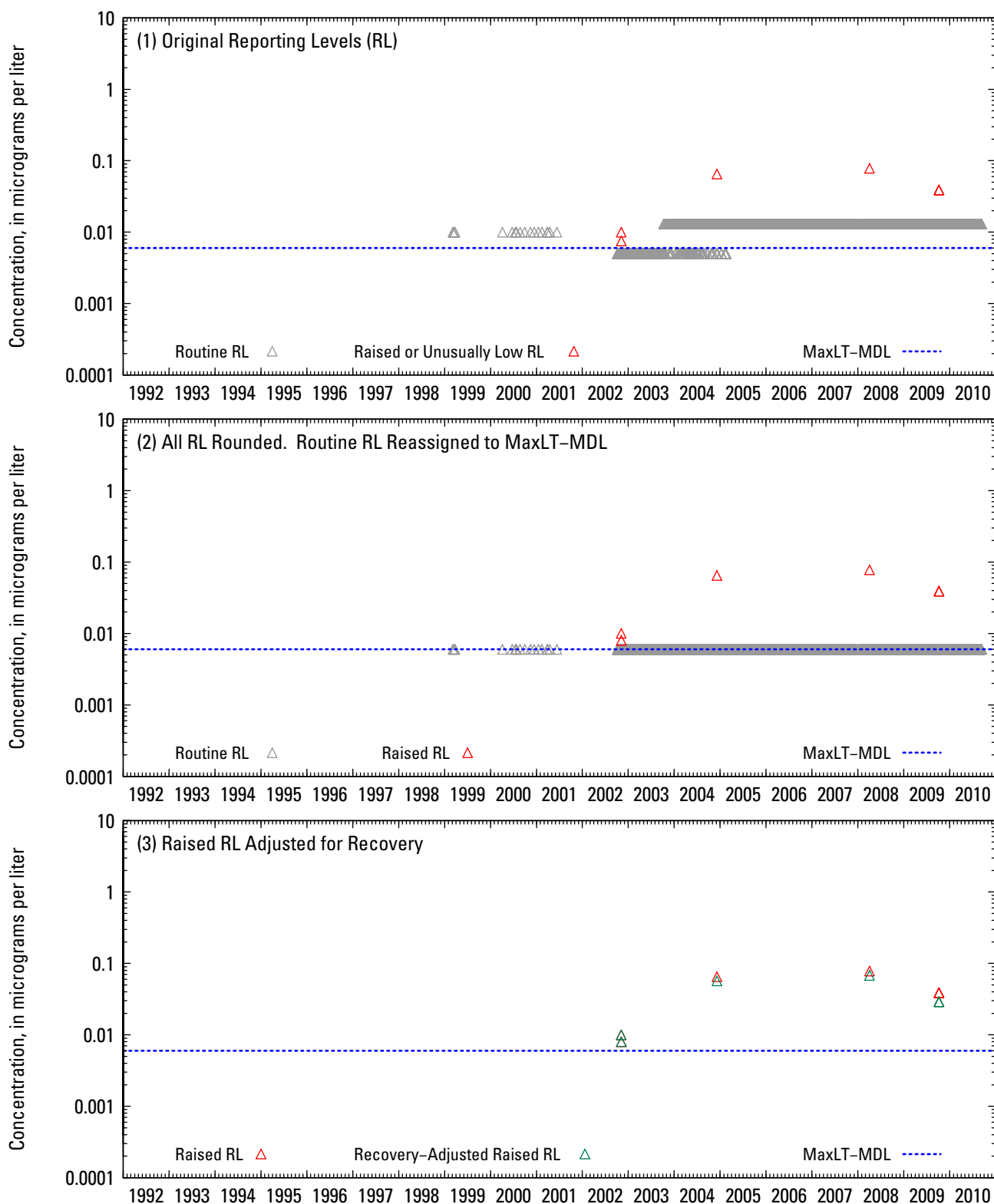
Figure 1–22. Time–series plots of nondetections of ethoprophos for all sites in the trend dataset showing (1) original reporting levels; (2) rounded reporting levels and, for routine nondetections, reporting levels reassigned to the maximum value of the long–term method detection level (maxLT–MDL); and (3) raised reporting levels adjusted for temporal changes in recovery. Temporal changes in recovery are shown in panel 2 of the figures in appendix 2.

Figure 1–23. Time–series plots of nondetections of fipronil for all sites in the trend dataset showing (1) original reporting levels; (2) rounded reporting levels and, for routine nondetections, reporting levels reassigned to the maximum value of the long–term method detection level (maxLT–MDL); and (3) raised reporting levels adjusted for temporal changes in recovery. Temporal changes in recovery are shown in panel 2 of the figures in appendix 2.
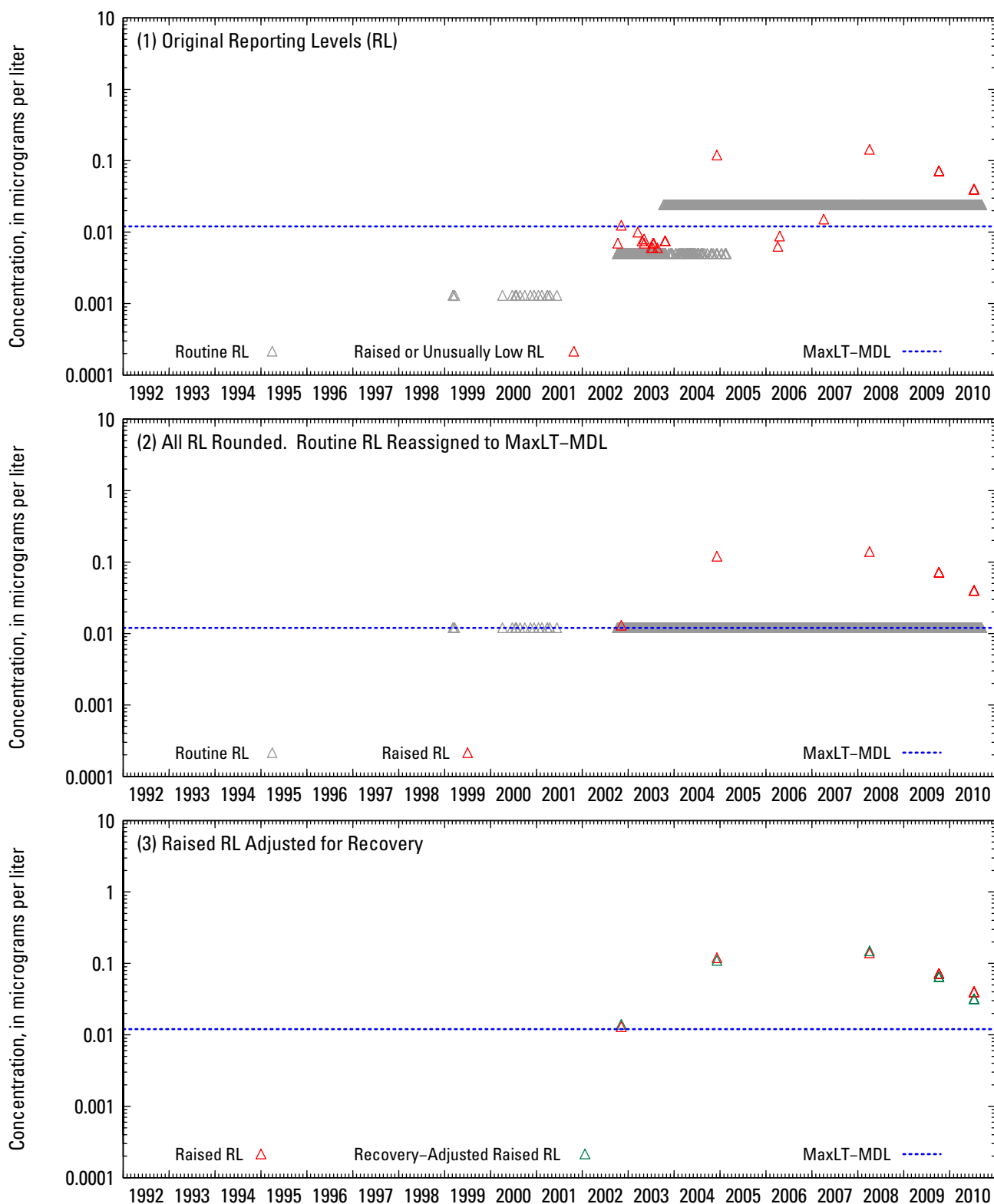
Figure 1–24. Time–series plots of nondetections of fipronil sulfide for all sites in the trend dataset showing (1) original reporting levels; (2) rounded reporting levels and, for routine nondetections, reporting levels reassigned to the maximum value of the long–term method detection level (maxLT–MDL); and (3) raised reporting levels adjusted for temporal changes in recovery. Temporal changes in recovery are shown in panel 2 of the figures in appendix 2.
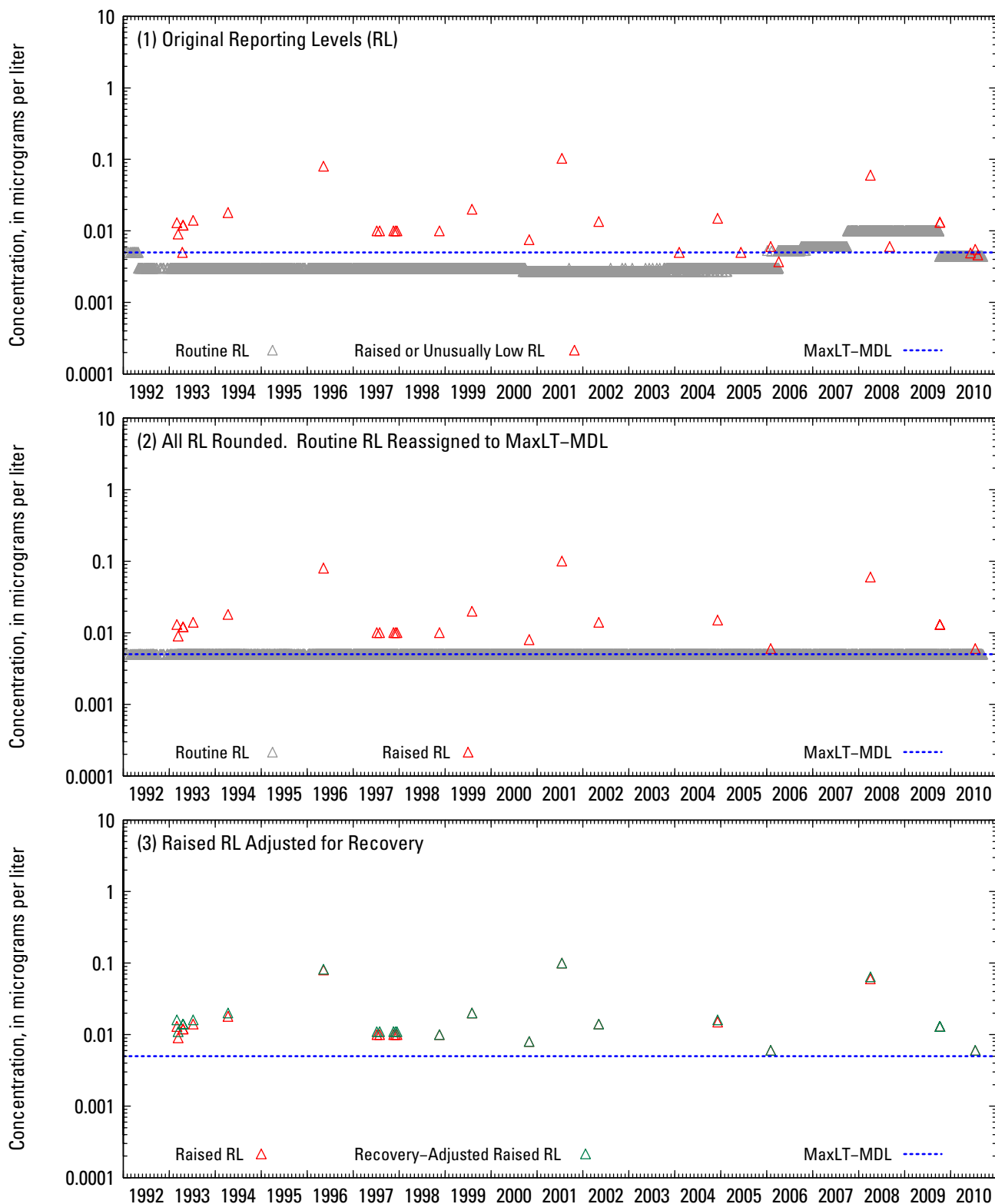
Figure 1–25. Time–series plots of nondetections of fipronil sulfone for all sites in the trend dataset showing (1) original reporting levels; (2) rounded reporting levels and, for routine nondetections, reporting levels reassigned to the maximum value of the long–term method detection level (maxLT–MDL); and (3) raised reporting levels adjusted for temporal changes in recovery. Temporal changes in recovery are shown in panel 2 of the figures in appendix 2.
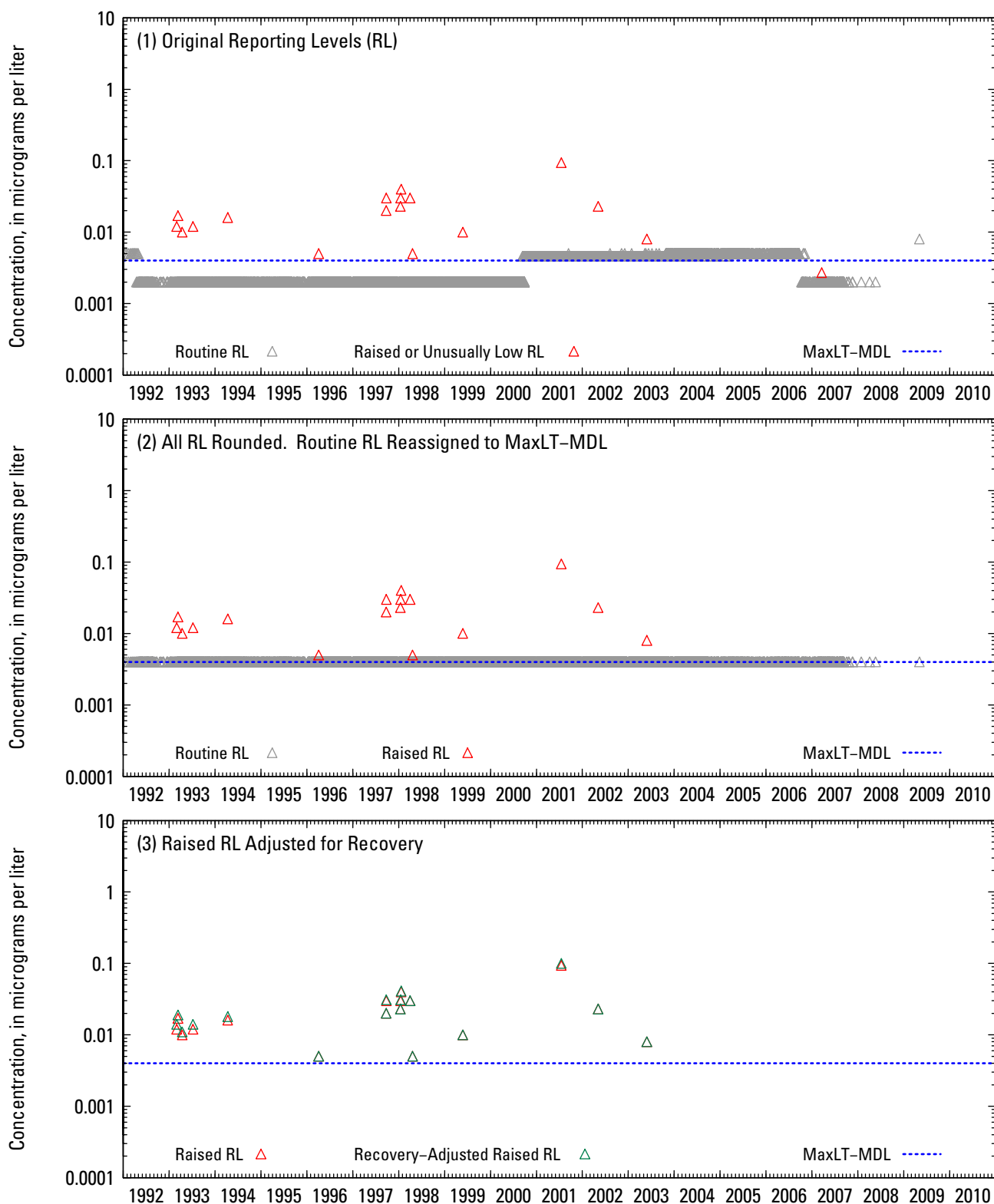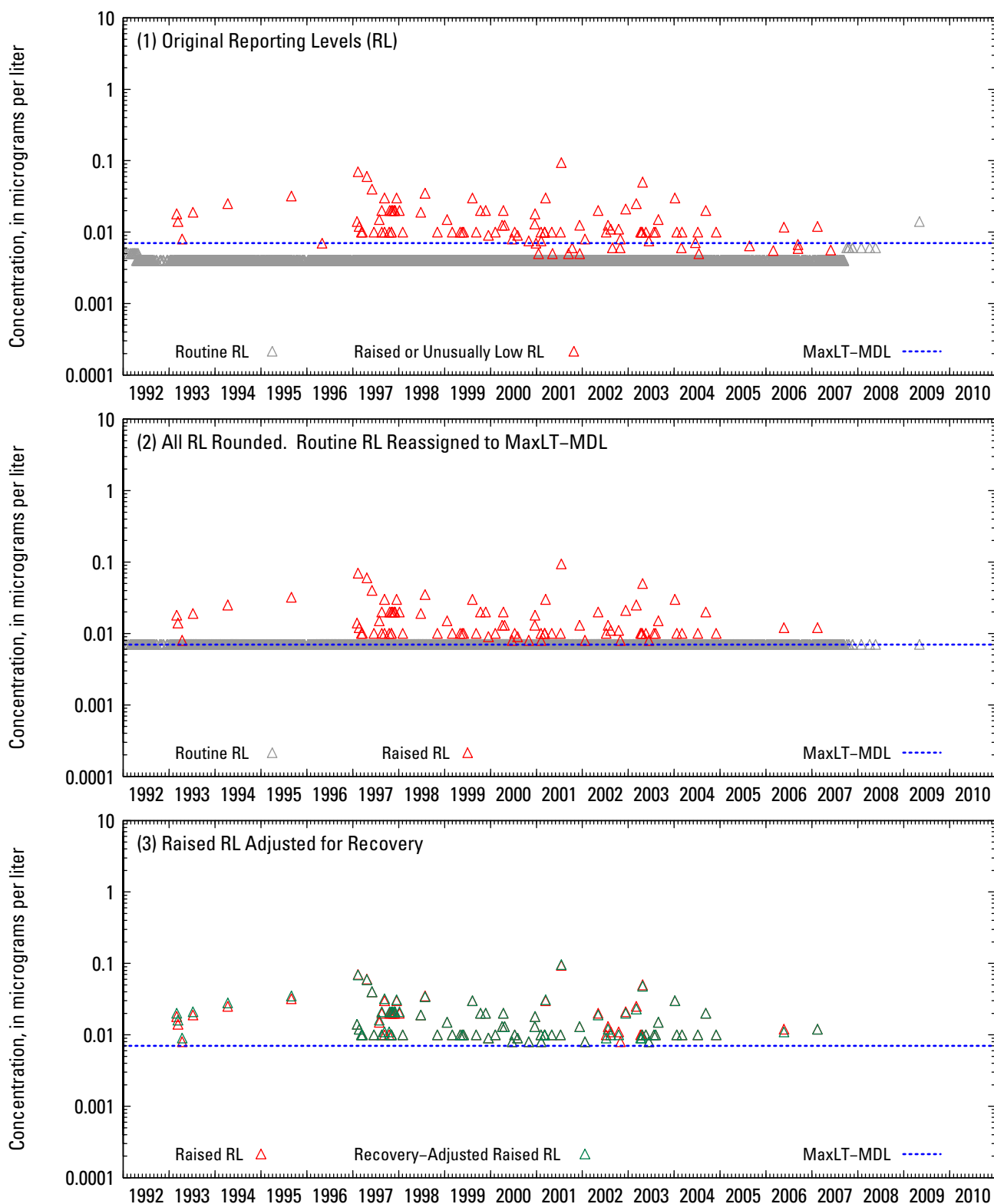
Figure 1–26. Time–series plots of nondetections of fonofos for all sites in the trend dataset showing (1) original reporting levels; (2) rounded reporting levels and, for routine nondetections, reporting levels reassigned to the maximum value of the long–term method detection level (maxLT–MDL); and (3) raised reporting levels adjusted for temporal changes in recovery. Temporal changes in recovery are shown in panel 2 of the figures in appendix 2.
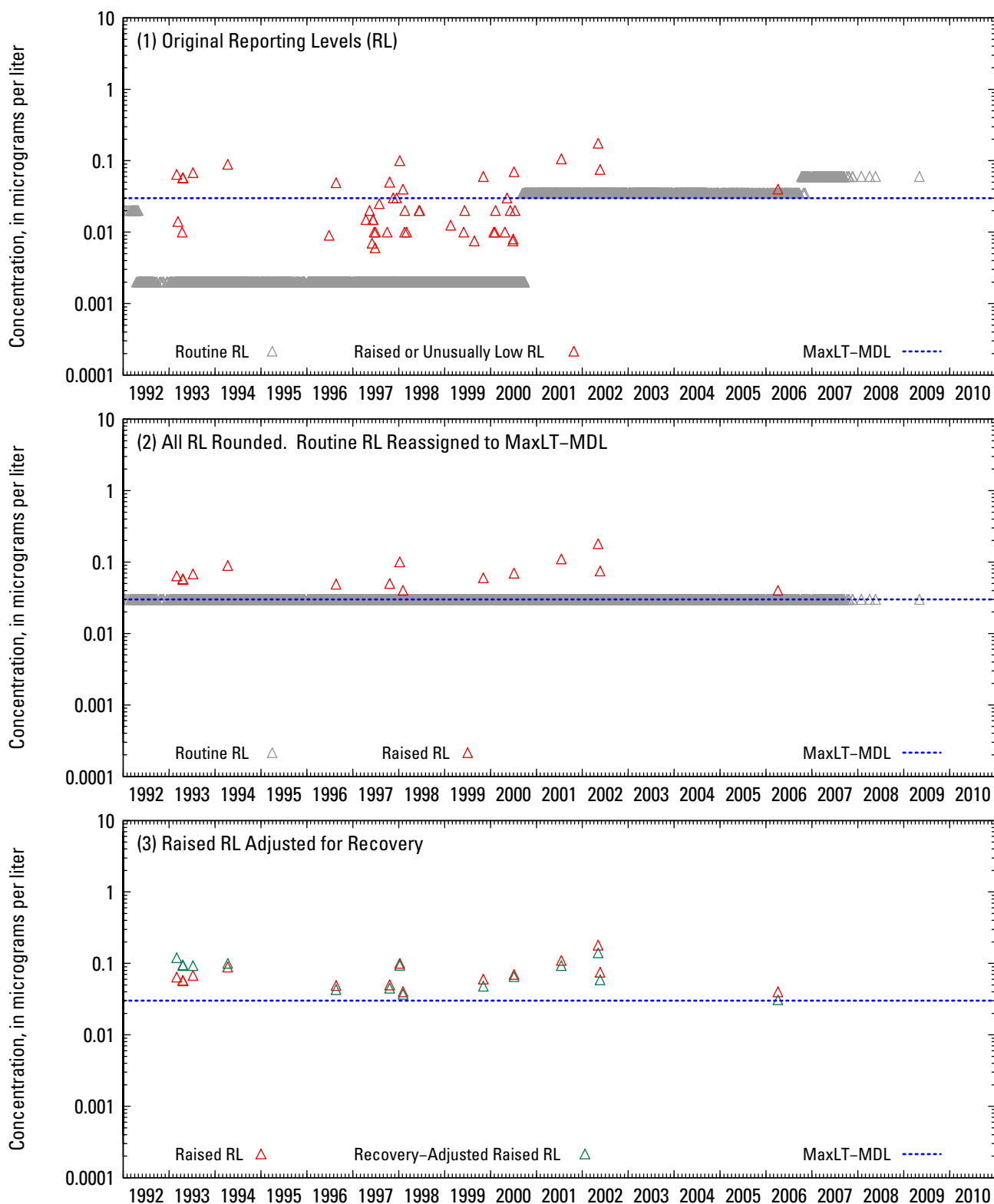
Figure 1–27. Time–series plots of nondetections of alpha–HCH for all sites in the trend dataset showing (1) original reporting levels; (2) rounded reporting levels and, for routine nondetections, reporting levels reassigned to the maximum value of the long–term method detection level (maxLT–MDL); and (3) raised reporting levels adjusted for temporal changes in recovery. Temporal changes in recovery are shown in panel 2 of the figures in appendix 2.
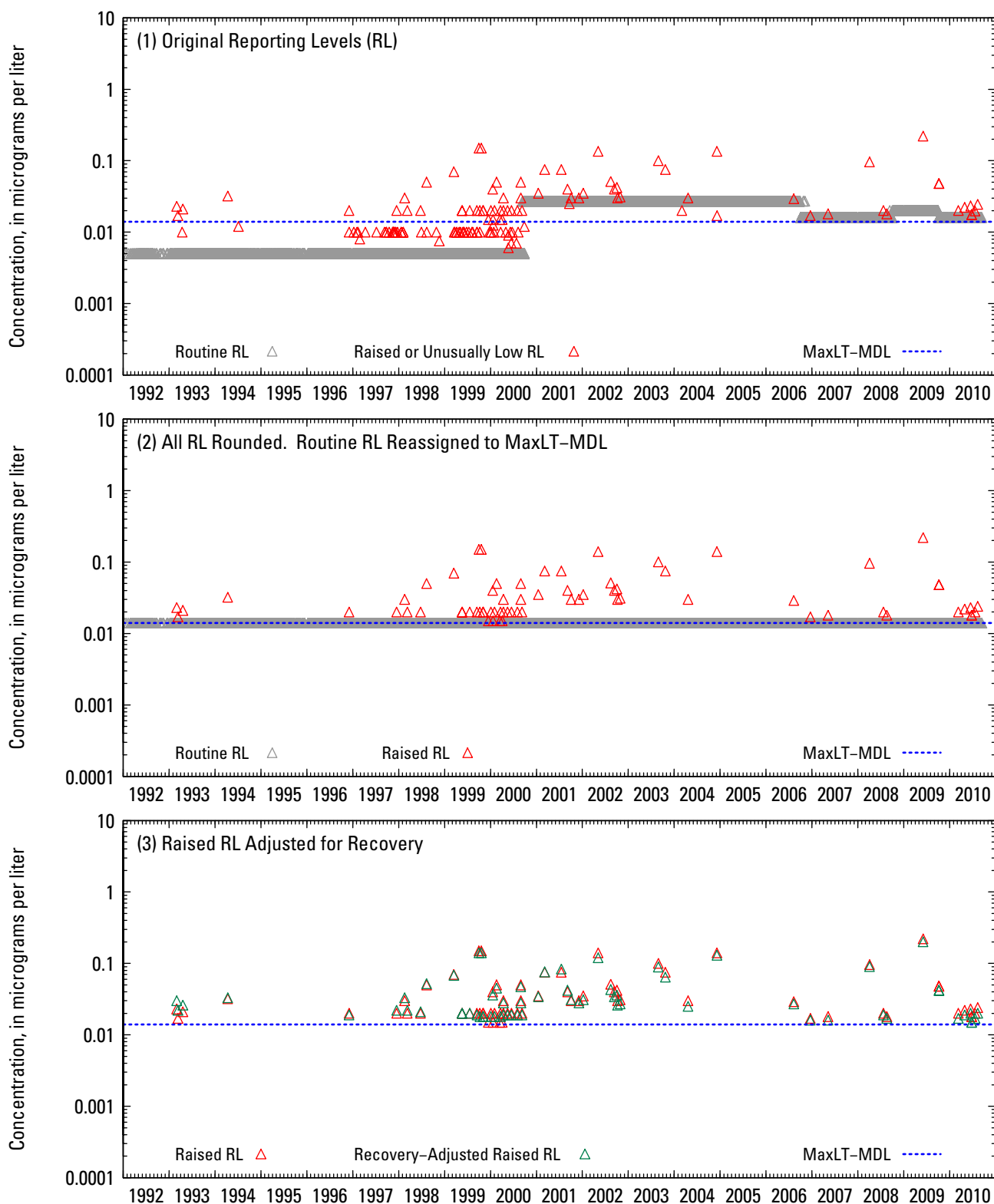
Figure 1–28. Time–series plots of nondetections of gamma–HCH for all sites in the trend dataset showing (1) original reporting levels; (2) rounded reporting levels and, for routine nondetections, reporting levels reassigned to the maximum value of the long–term method detection level (maxLT–MDL); and (3) raised reporting levels adjusted for temporal changes in recovery. Temporal changes in recovery are shown in panel 2 of the figures in appendix 2.
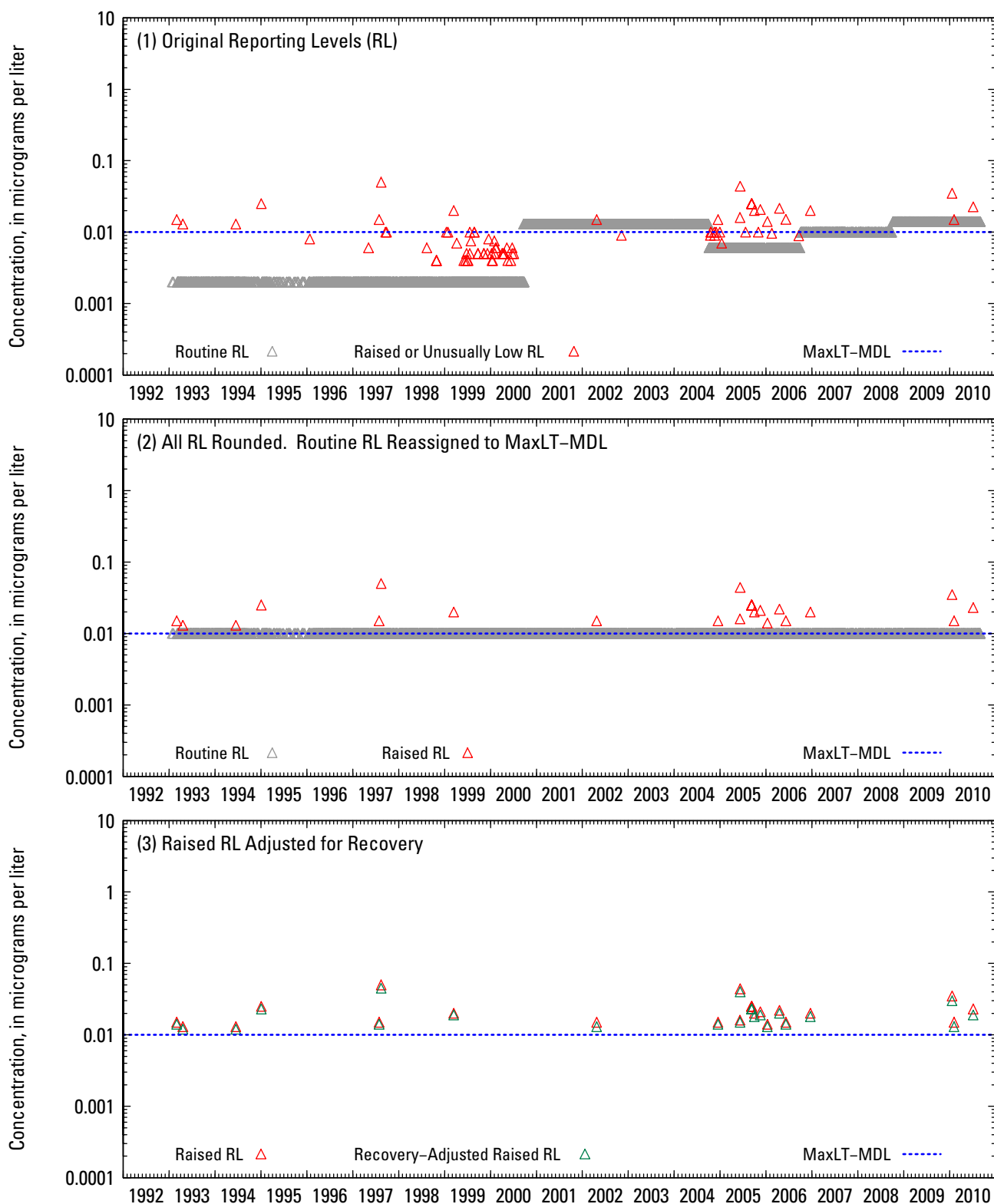
Figure 1–29. Time–series plots of nondetections of linuron for all sites in the trend dataset showing (1) original reporting levels; (2) rounded reporting levels and, for routine nondetections, reporting levels reassigned to the maximum value of the long–term method detection level (maxLT–MDL); and (3) raised reporting levels adjusted for temporal changes in recovery. Temporal changes in recovery are shown in panel 2 of the figures in appendix 2.
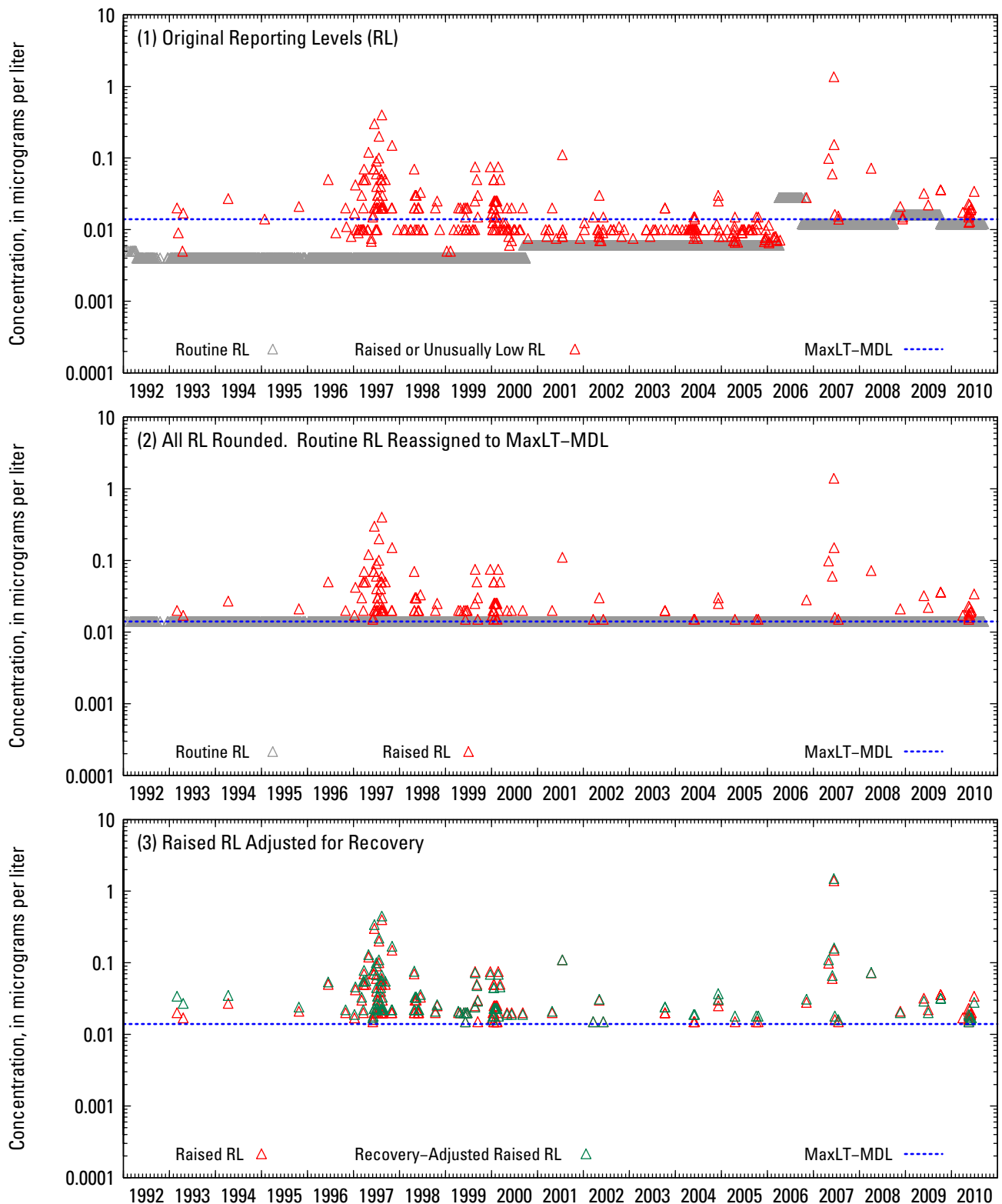
Figure 1–30. Time–series plots of nondetections of malathion for all sites in the trend dataset showing (1) original reporting levels; (2) rounded reporting levels and, for routine nondetections, reporting levels reassigned to the maximum value of the long–term method detection level (maxLT–MDL); and (3) raised reporting levels adjusted for temporal changes in recovery. Temporal changes in recovery are shown in panel 2 of the figures in appendix 2.

Figure 1–31. Time–series plots of nondetections of metolachlor for all sites in the trend dataset showing (1) original reporting levels; (2) rounded reporting levels and, for routine nondetections, reporting levels reassigned to the maximum value of the long–term method detection level (maxLT–MDL); and (3) raised reporting levels adjusted for temporal changes in recovery. Temporal changes in recovery are shown in panel 2 of the figures in appendix 2.
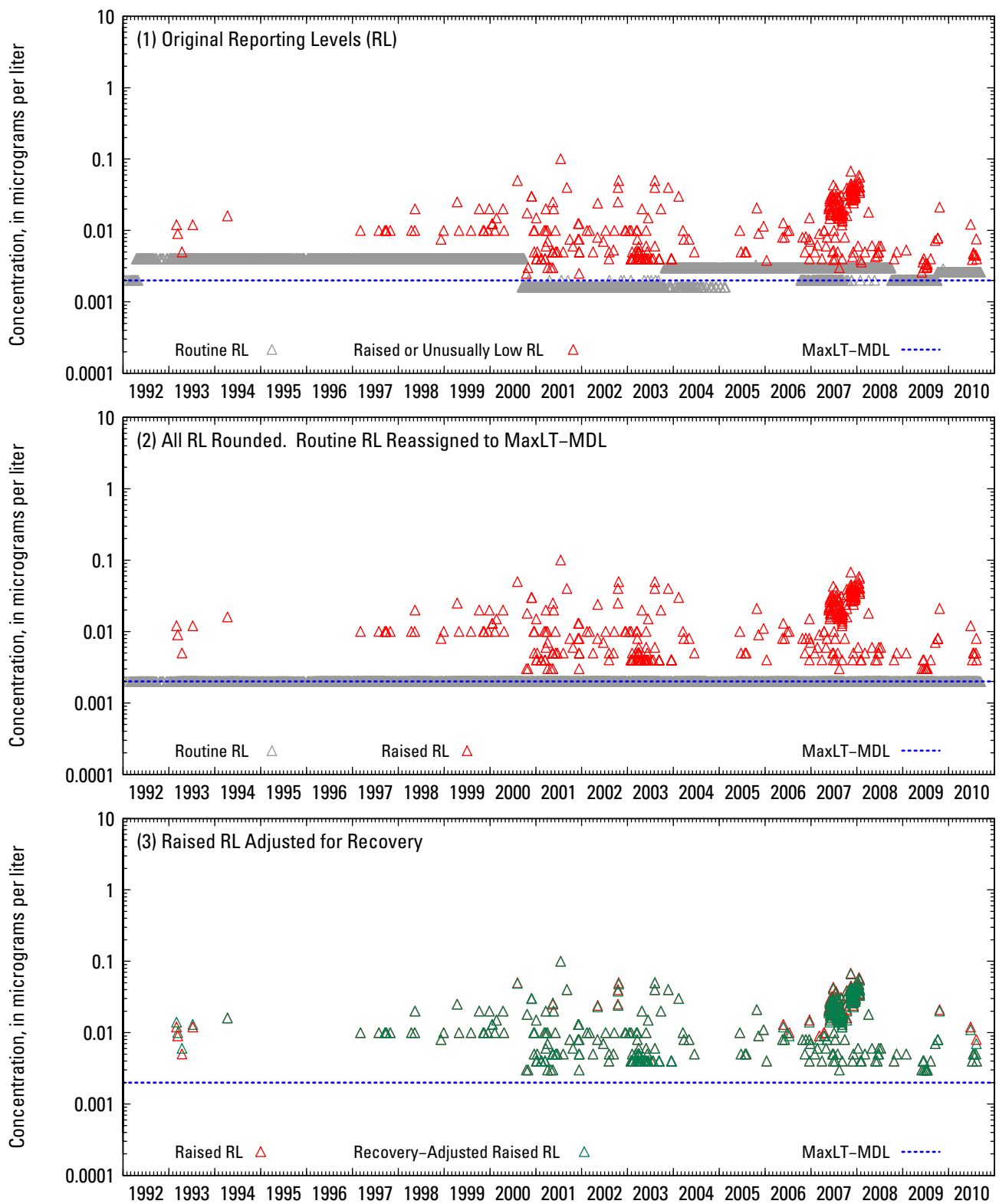
Figure 1–32. Time–series plots of nondetections of metribuzin for all sites in the trend dataset showing (1) original reporting levels; (2) rounded reporting levels and, for routine nondetections, reporting levels reassigned to the maximum value of the long–term method detection level (maxLT–MDL); and (3) raised reporting levels adjusted for temporal changes in recovery. Temporal changes in recovery are shown in panel 2 of the figures in appendix 2.
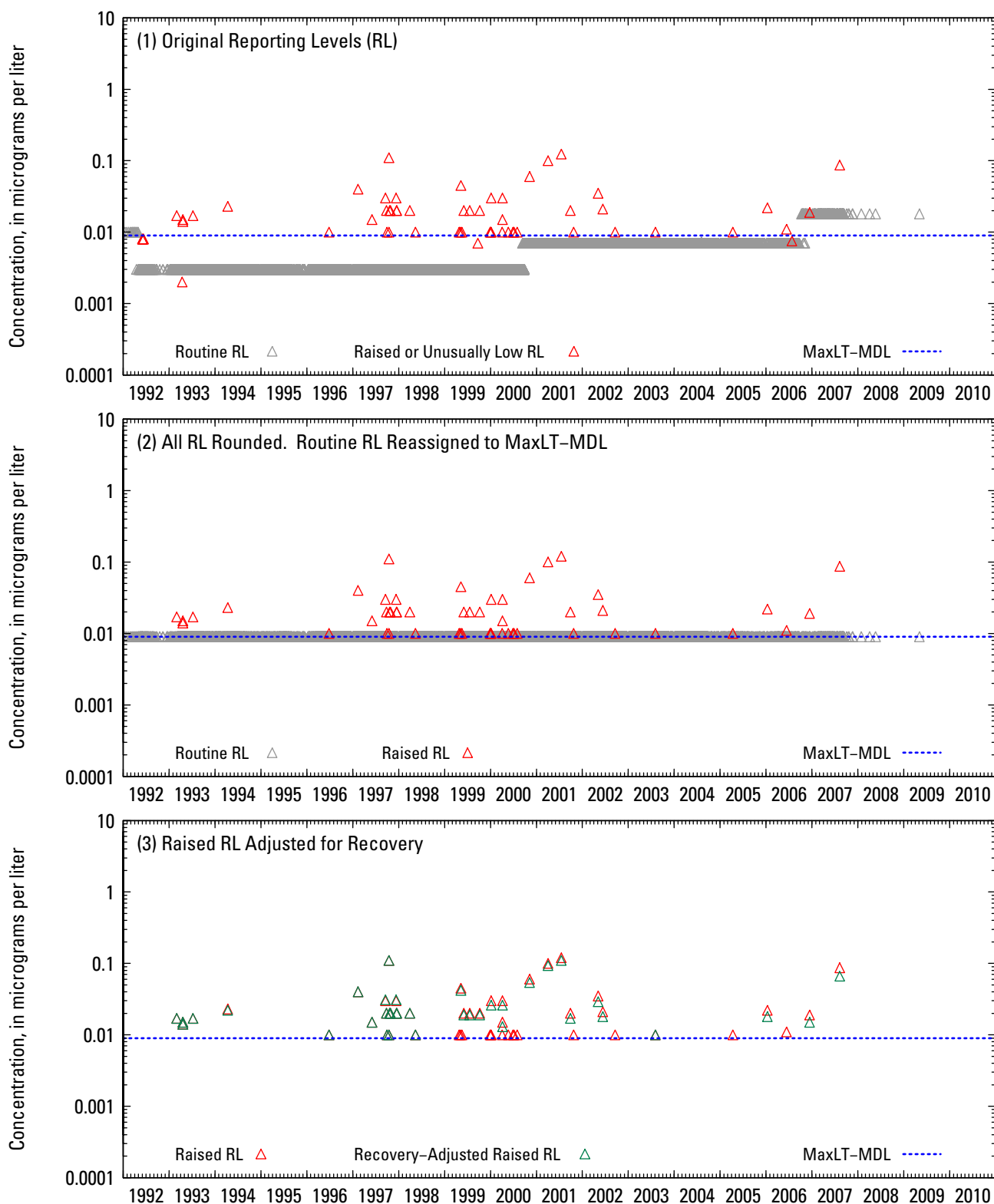
Figure 1–33. Time–series plots of nondetections of molinate for all sites in the trend dataset showing (1) original reporting levels; (2) rounded reporting levels and, for routine nondetections, reporting levels reassigned to the maximum value of the long–term method detection level (maxLT–MDL); and (3) raised reporting levels adjusted for temporal changes in recovery. Temporal changes in recovery are shown in panel 2 of the figures in appendix 2.
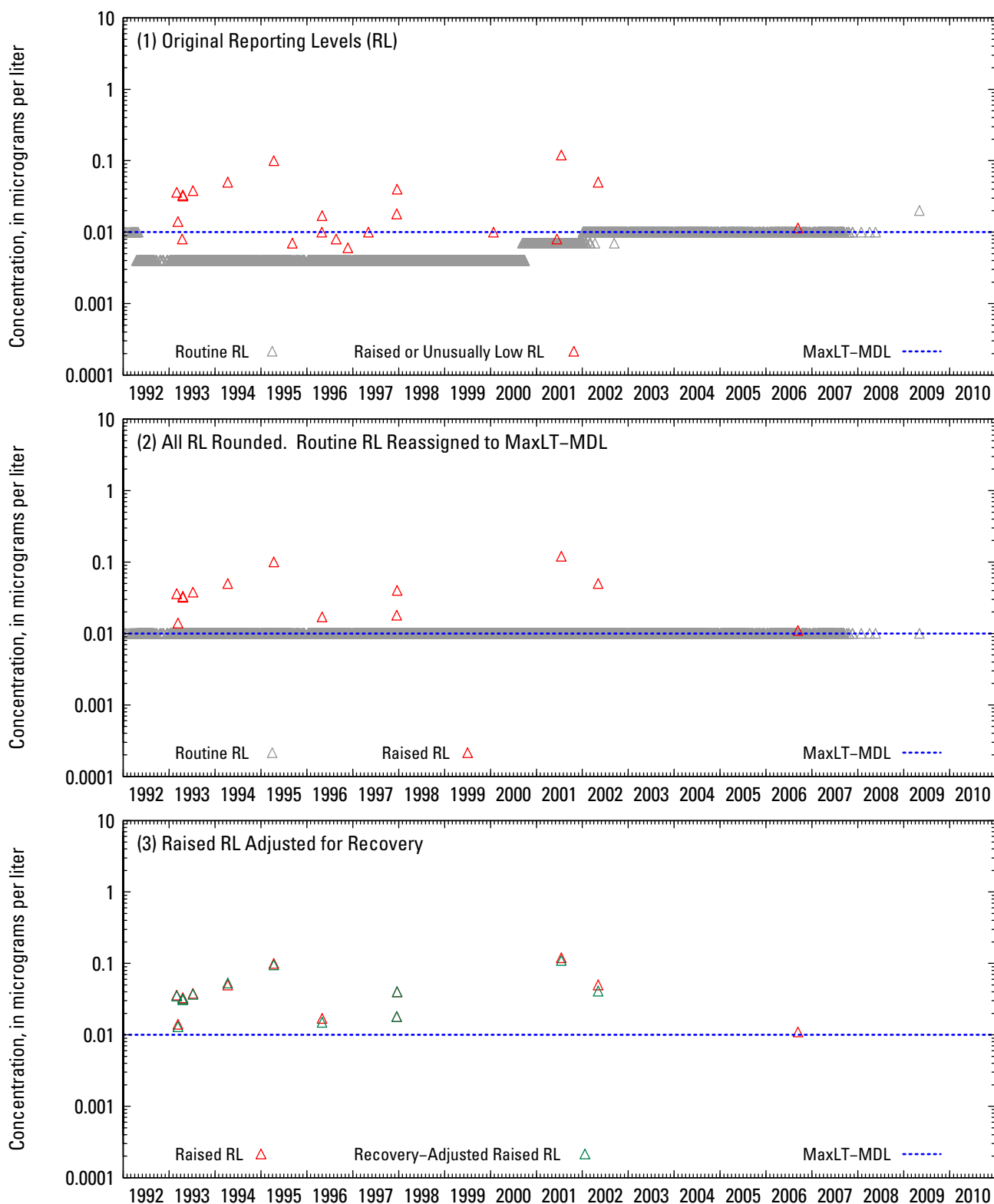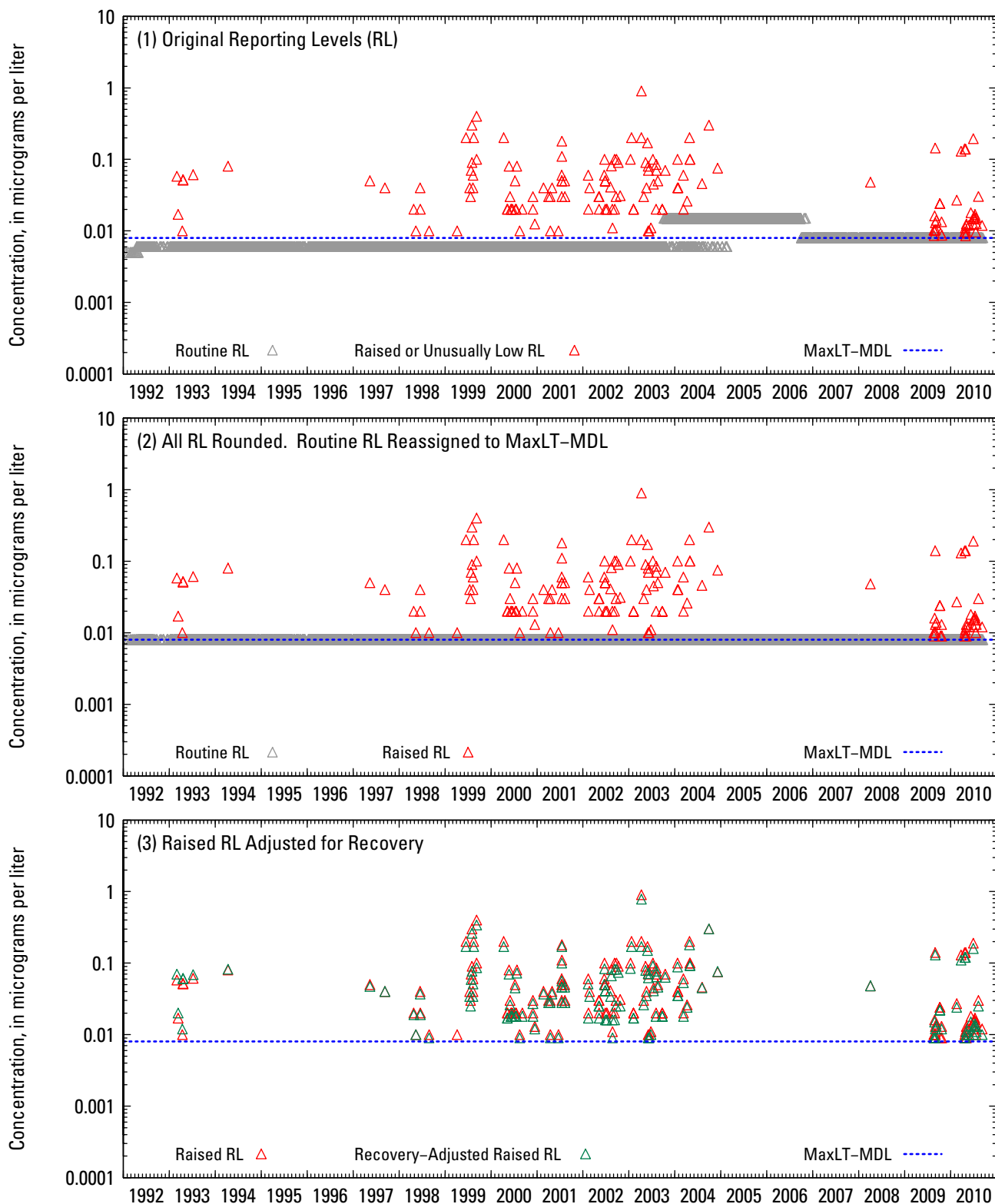
Figure 1–34. Time–series plots of nondetections of napropamide for all sites in the trend dataset showing (1) original reporting levels; (2) rounded reporting levels and, for routine nondetections, reporting levels reassigned to the maximum value of the long–term method detection level (maxLT–MDL); and (3) raised reporting levels adjusted for temporal changes in recovery. Temporal changes in recovery are shown in panel 2 of the figures in appendix 2.
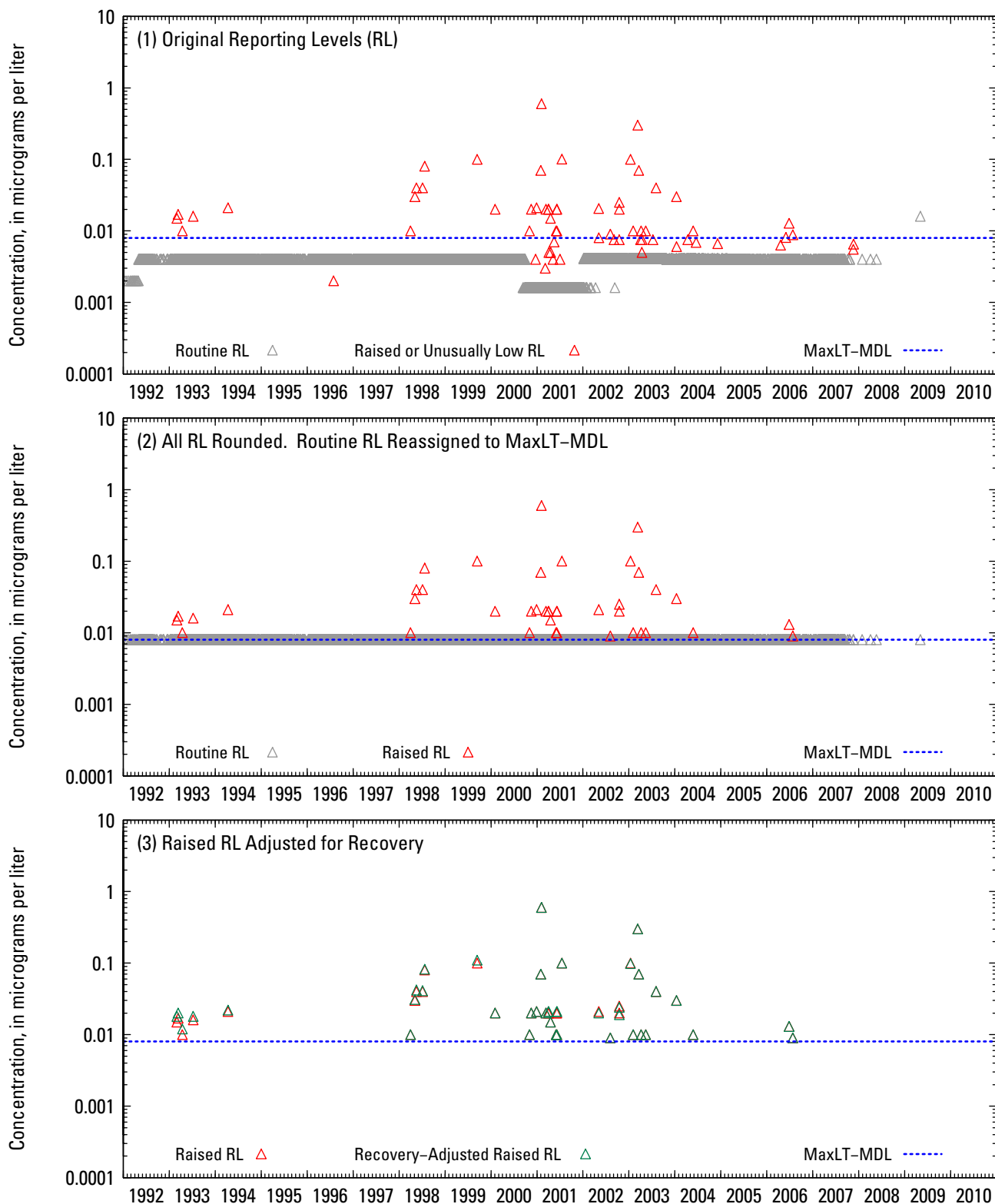
Figure 1–35. Time–series plots of nondetections of parathion for all sites in the trend dataset showing (1) original reporting levels; (2) rounded reporting levels and, for routine nondetections, reporting levels reassigned to the maximum value of the long–term method detection level (maxLT–MDL); and (3) raised reporting levels adjusted for temporal changes in recovery. Temporal changes in recovery are shown in panel 2 of the figures in appendix 2.
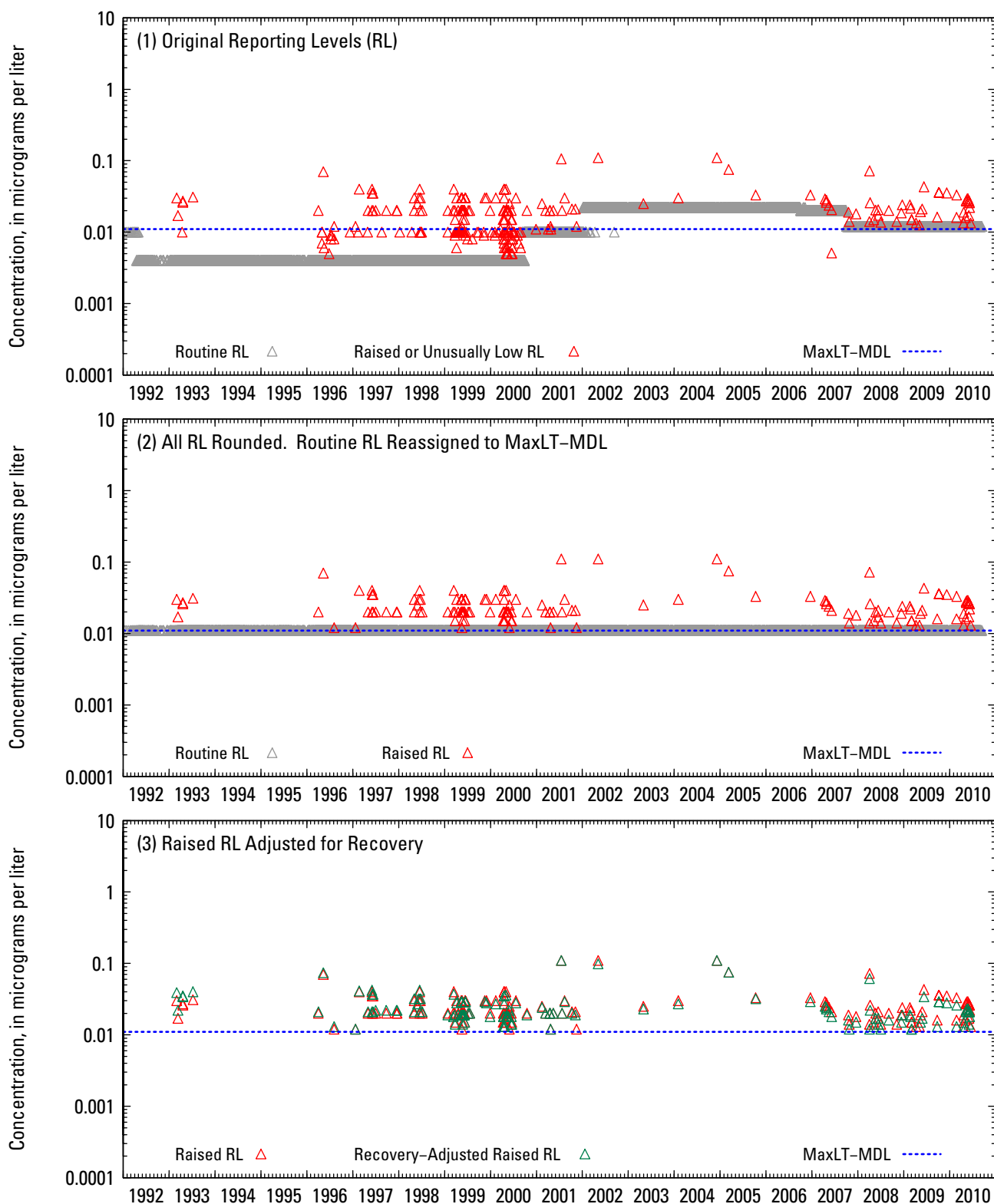
Figure 1–36. Time–series plots of nondetections of parathion–methyl for all sites in the trend dataset showing (1) original reporting levels; (2) rounded reporting levels and, for routine nondetections, reporting levels reassigned to the maximum value of the long–term method detection level (maxLT–MDL); and (3) raised reporting levels adjusted for temporal changes in recovery. Temporal changes in recovery are shown in panel 2 of the figures in appendix 2.
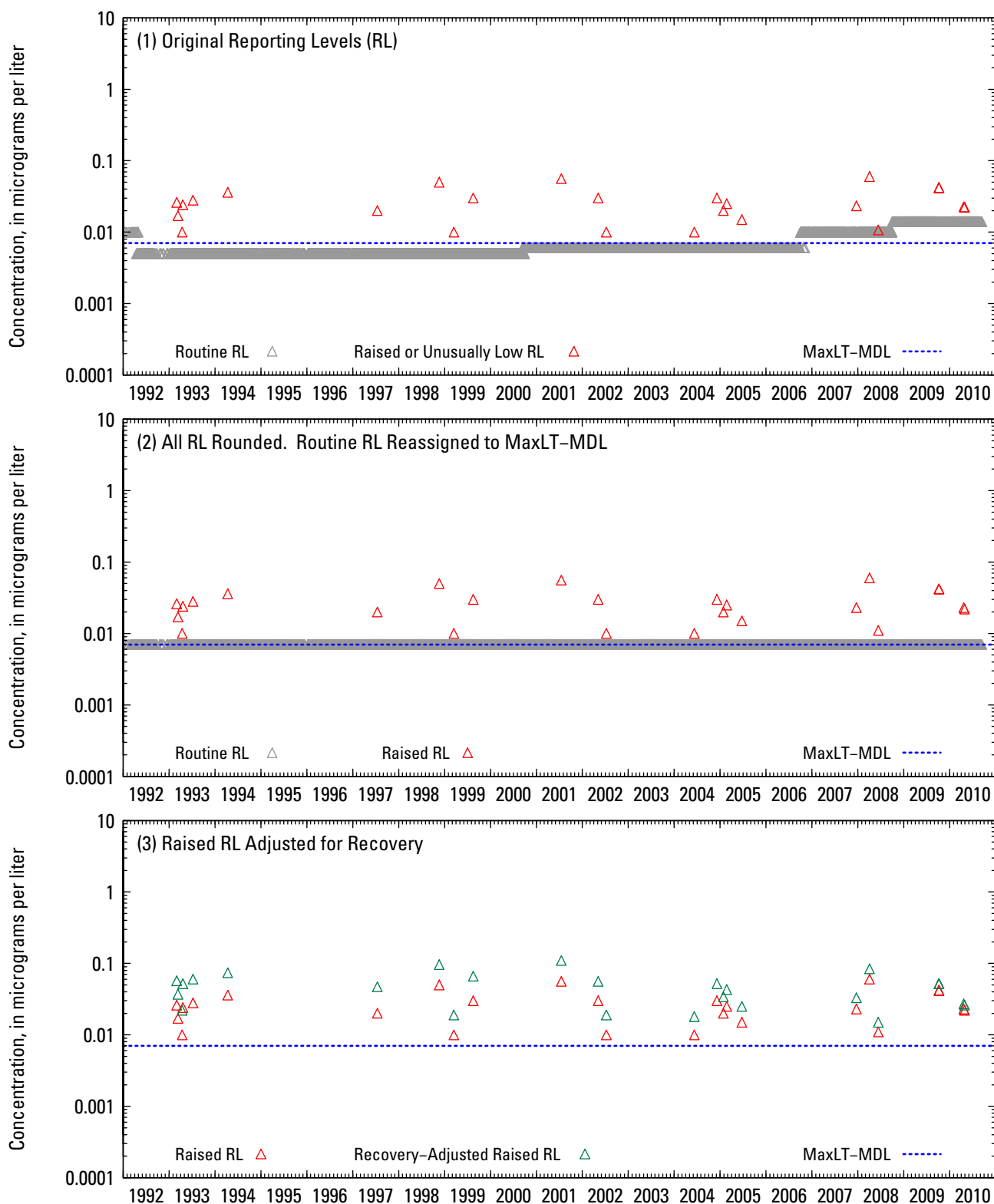
Figure 1–37. Time–series plots of nondetections of pebulate for all sites in the trend dataset showing (1) original reporting levels; (2) rounded reporting levels and, for routine nondetections, reporting levels reassigned to the maximum value of the long–term method detection level (maxLT–MDL); and (3) raised reporting levels adjusted for temporal changes in recovery. Temporal changes in recovery are shown in panel 2 of the figures in appendix 2.
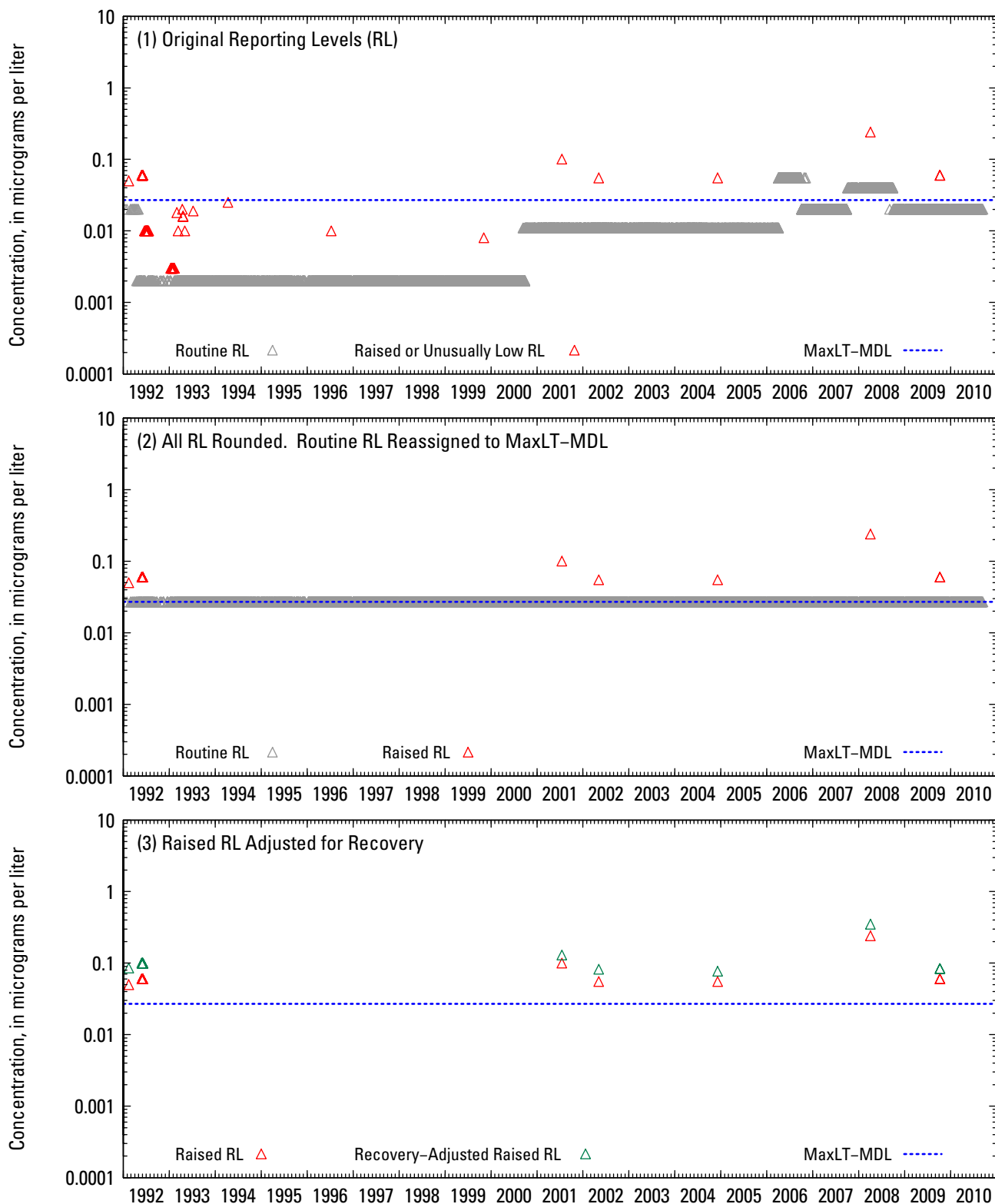
Figure 1–38. Time–series plots of nondetections of pendimethalin for all sites in the trend dataset showing (1) original reporting levels; (2) rounded reporting levels and, for routine nondetections, reporting levels reassigned to the maximum value of the long–term method detection level (maxLT–MDL); and (3) raised reporting levels adjusted for temporal changes in recovery. Temporal changes in recovery are shown in panel 2 of the figures in appendix 2.

Figure 1–39. Time–series plots of nondetections of cis–permethrin for all sites in the trend dataset showing (1) original reporting levels; (2) rounded reporting levels and, for routine nondetections, reporting levels reassigned to the maximum value of the long–term method detection level (maxLT–MDL); and (3) raised reporting levels adjusted for temporal changes in recovery. Temporal changes in recovery are shown in panel 2 of the figures in appendix 2.
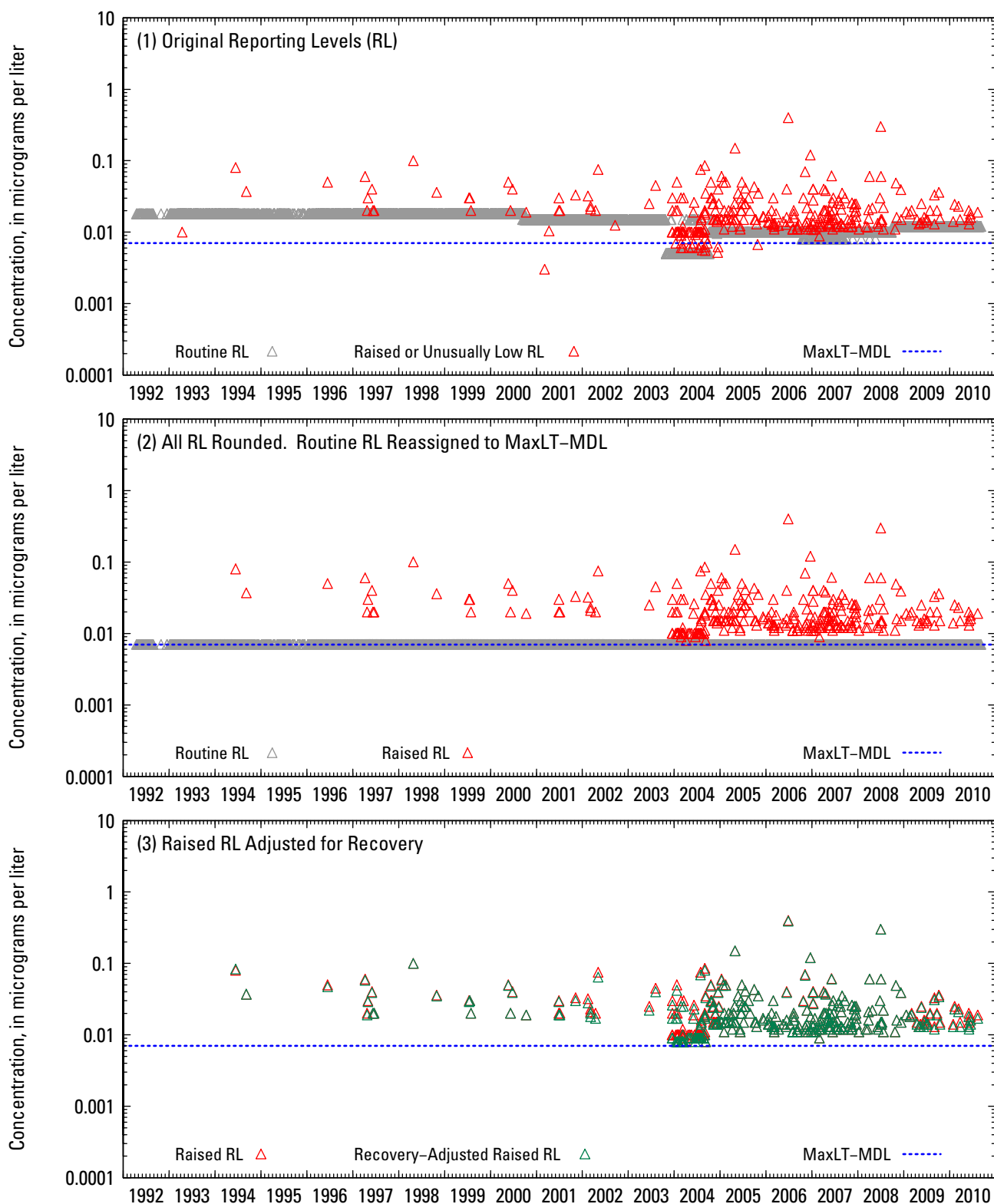
Figure 1–40. Time–series plots of nondetections of phorate for all sites in the trend dataset showing (1) original reporting levels; (2) rounded reporting levels and, for routine nondetections, reporting levels reassigned to the maximum value of the long–term method detection level (maxLT–MDL); and (3) raised reporting levels adjusted for temporal changes in recovery. Temporal changes in recovery are shown in panel 2 of the figures in appendix 2.
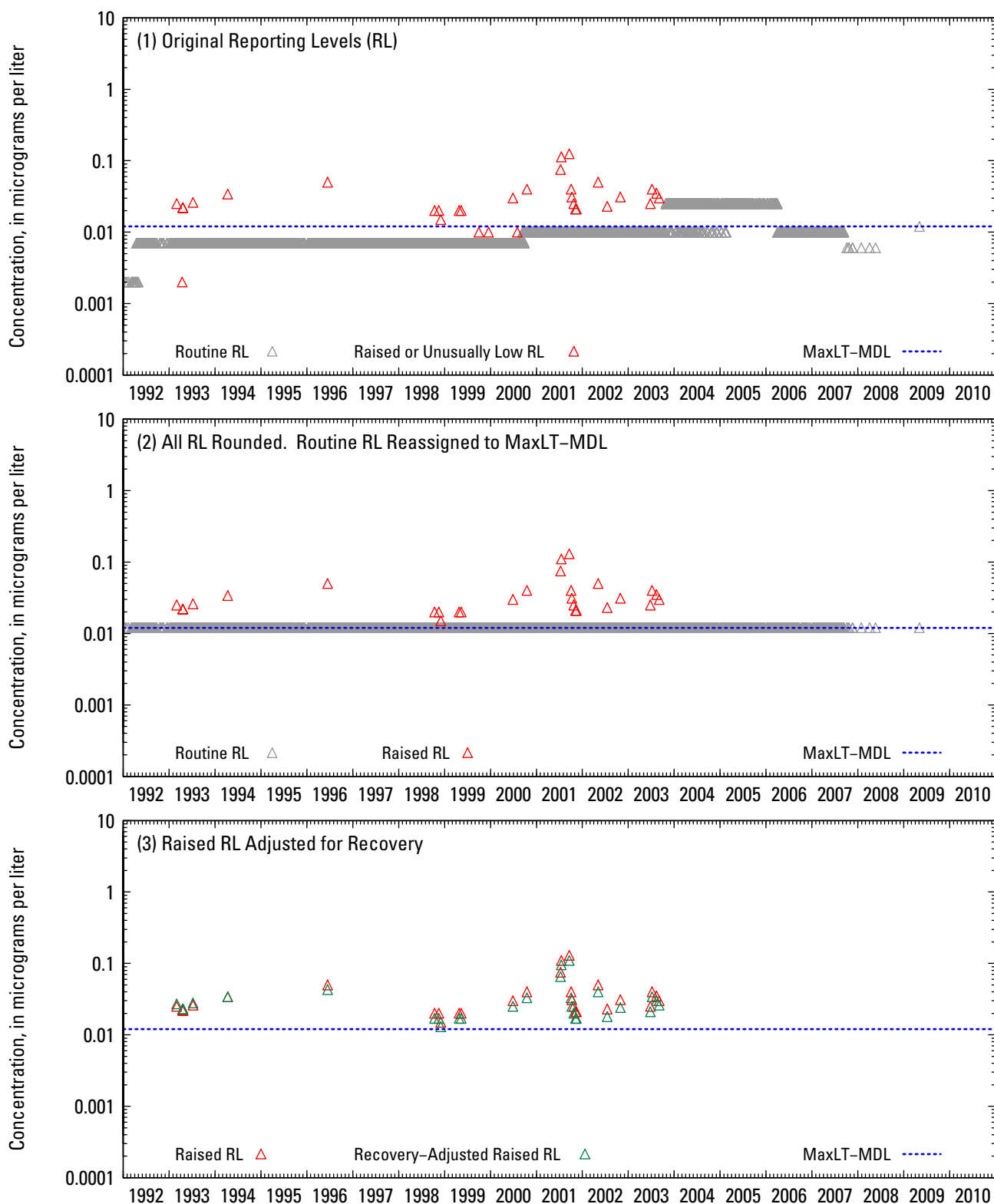
Figure 1–41. Time–series plots of nondetections of prometon for all sites in the trend dataset showing (1) original reporting levels; (2) rounded reporting levels and, for routine nondetections, reporting levels reassigned to the maximum value of the long–term method detection level (maxLT–MDL); and (3) raised reporting levels adjusted for temporal changes in recovery. Temporal changes in recovery are shown in panel 2 of the figures in appendix 2.
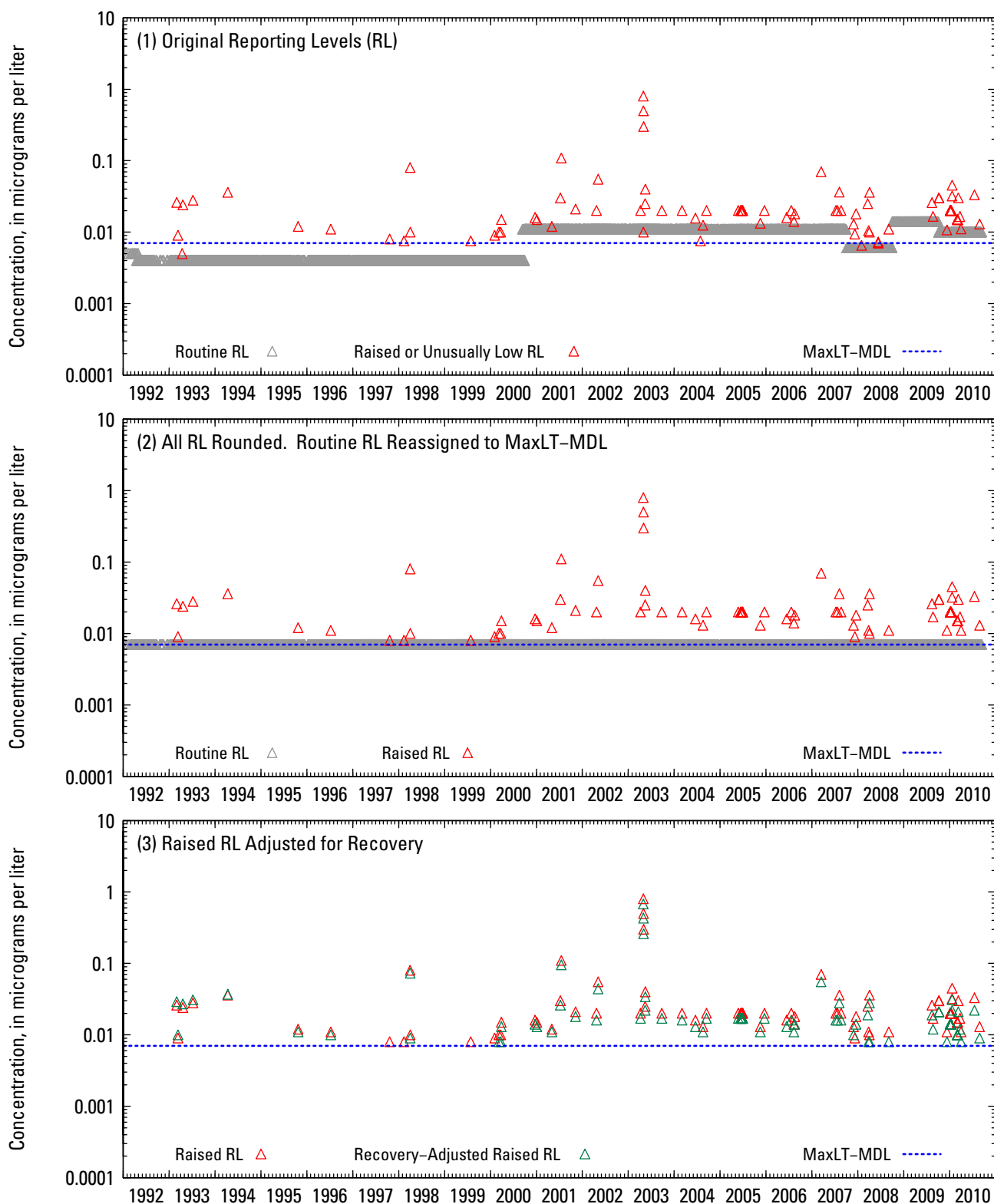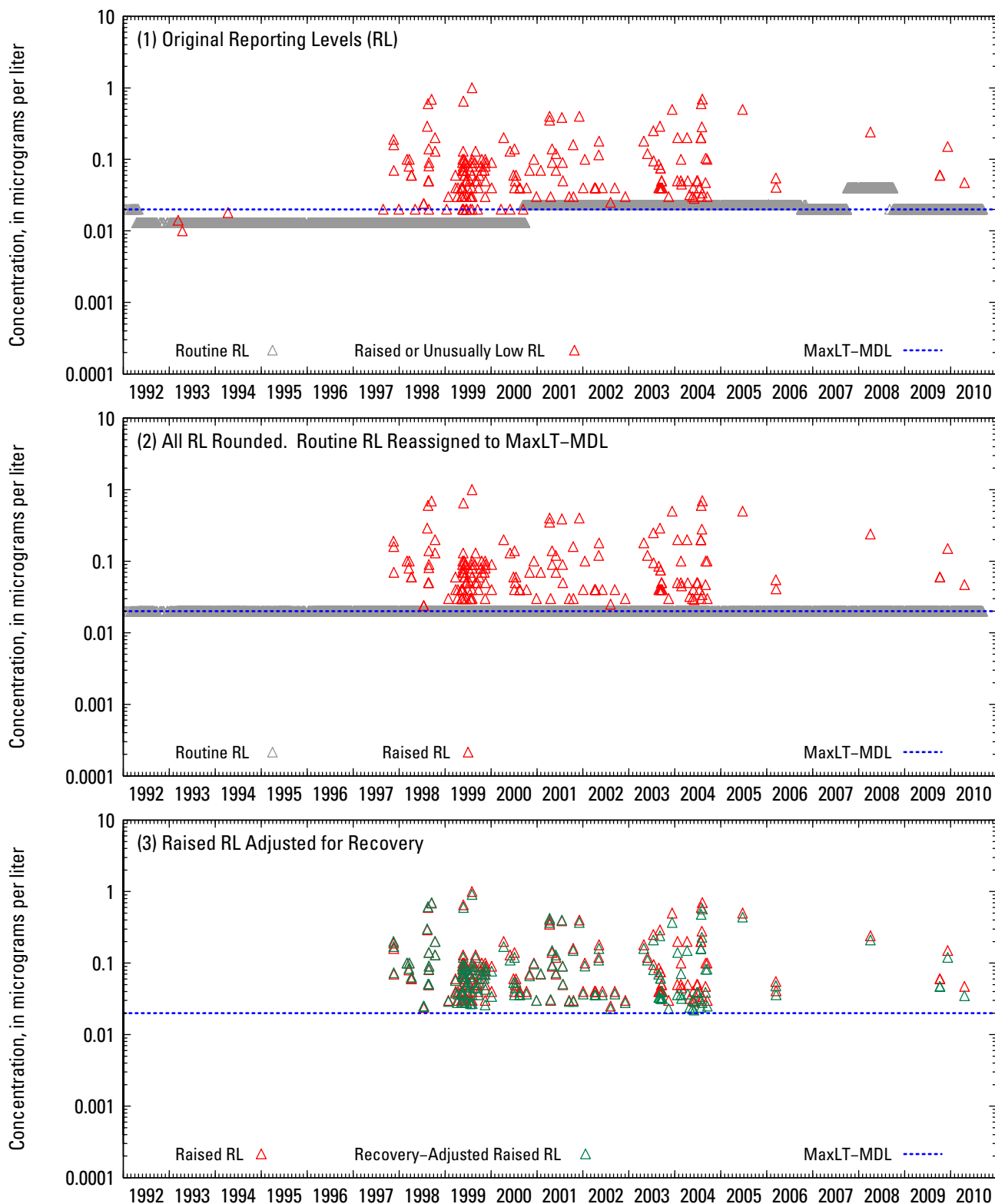
Figure 1–42. Time–series plots of nondetections of propachlor for all sites in the trend dataset showing (1) original reporting levels; (2) rounded reporting levels and, for routine nondetections, reporting levels reassigned to the maximum value of the long–term method detection level (maxLT–MDL); and (3) raised reporting levels adjusted for temporal changes in recovery. Temporal changes in recovery are shown in panel 2 of the figures in appendix 2.
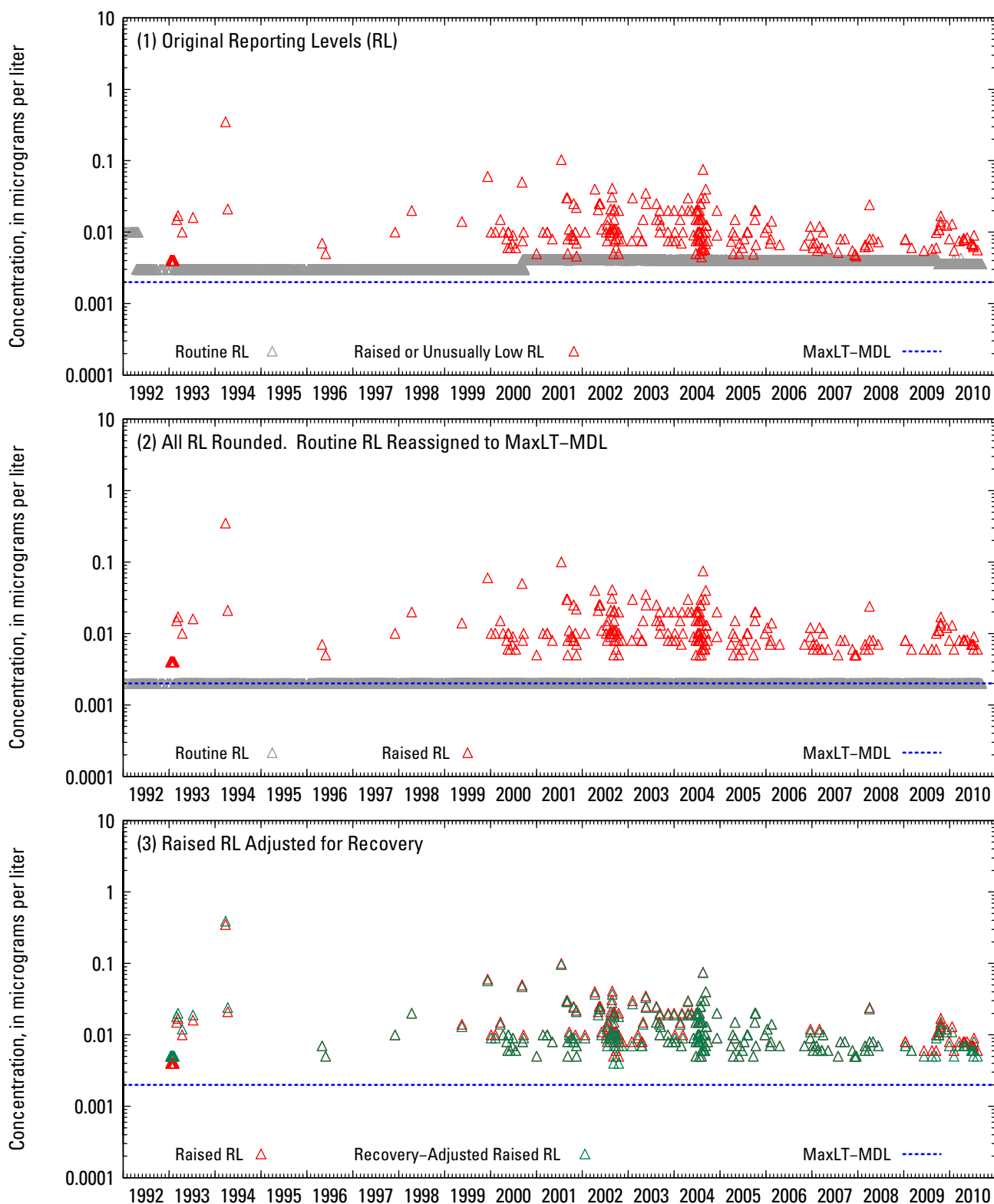
Figure 1–43. Time–series plots of nondetections of propanil for all sites in the trend dataset showing (1) original reporting levels; (2) rounded reporting levels and, for routine nondetections, reporting levels reassigned to the maximum value of the long–term method detection level (maxLT–MDL); and (3) raised reporting levels adjusted for temporal changes in recovery. Temporal changes in recovery are shown in panel 2 of the figures in appendix 2.
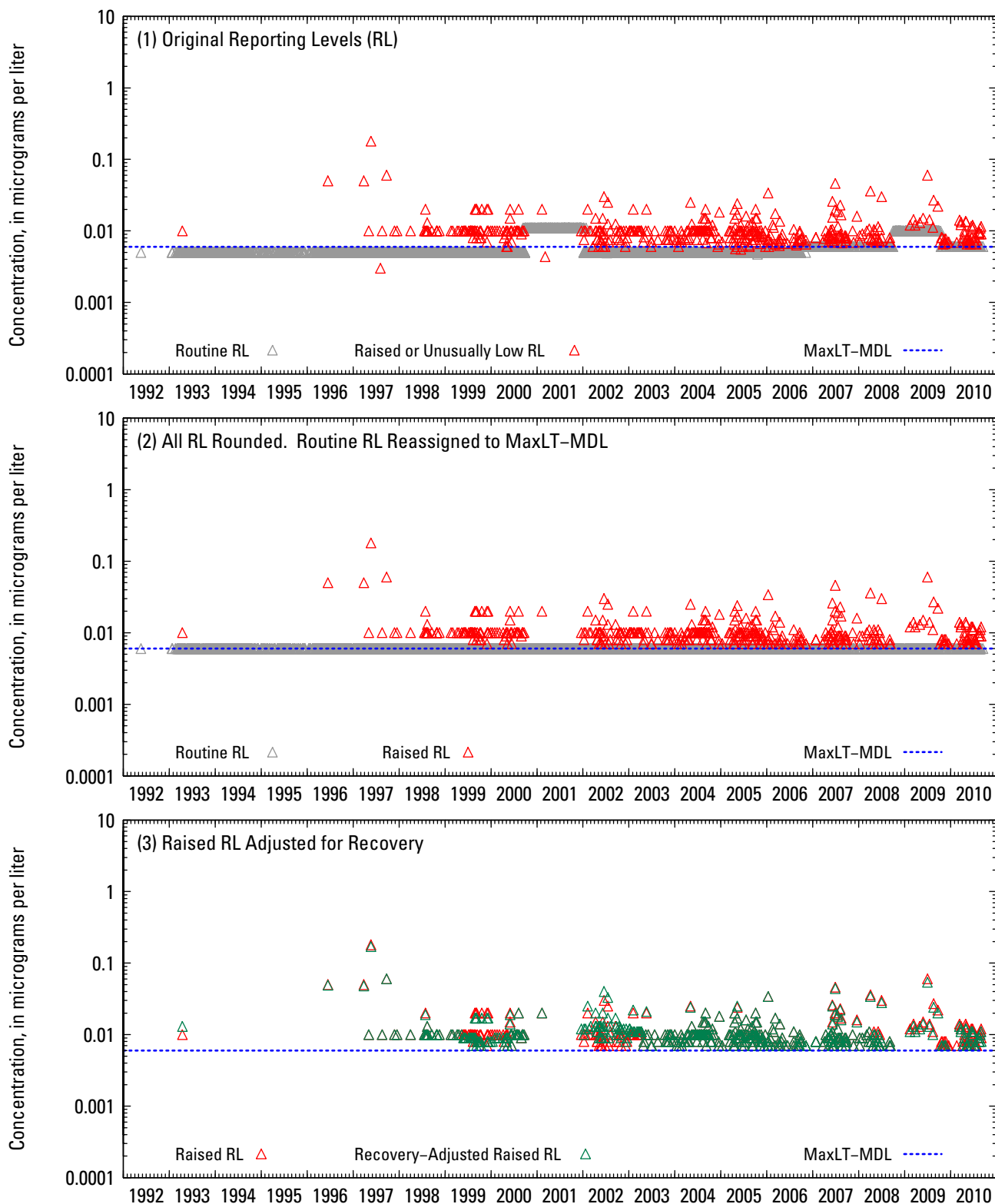
Figure 1–44. Time–series plots of nondetections of propargite for all sites in the trend dataset showing (1) original reporting levels; (2) rounded reporting levels and, for routine nondetections, reporting levels reassigned to the maximum value of the long–term method detection level (maxLT–MDL); and (3) raised reporting levels adjusted for temporal changes in recovery. Temporal changes in recovery are shown in panel 2 of the figures in appendix 2.
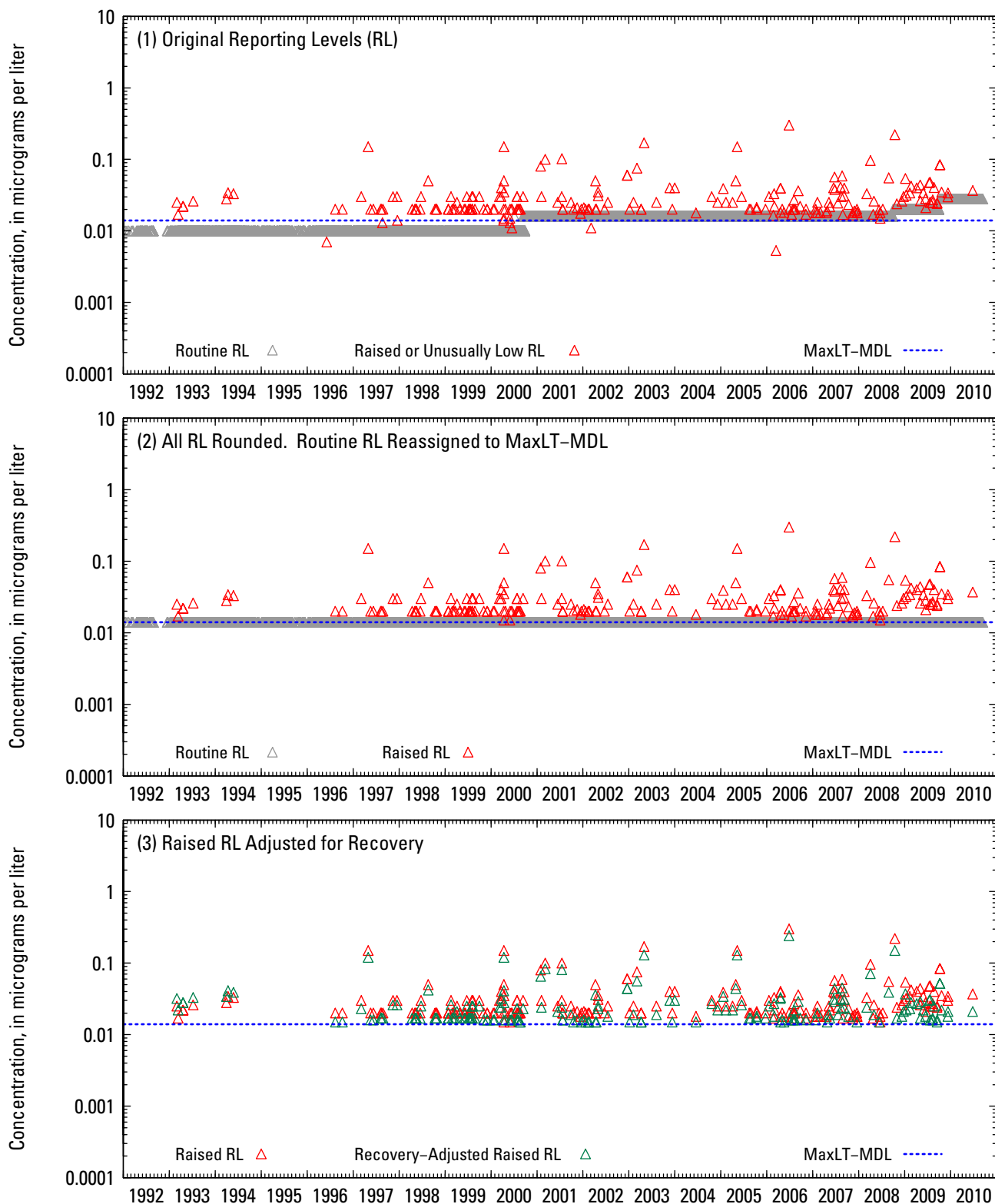
Figure 1–45. Time–series plots of nondetections of propyzamide for all sites in the trend dataset showing (1) original reporting levels; (2) rounded reporting levels and, for routine nondetections, reporting levels reassigned to the maximum value of the long–term method detection level (maxLT–MDL); and (3) raised reporting levels adjusted for temporal changes in recovery. Temporal changes in recovery are shown in panel 2 of the figures in appendix 2.
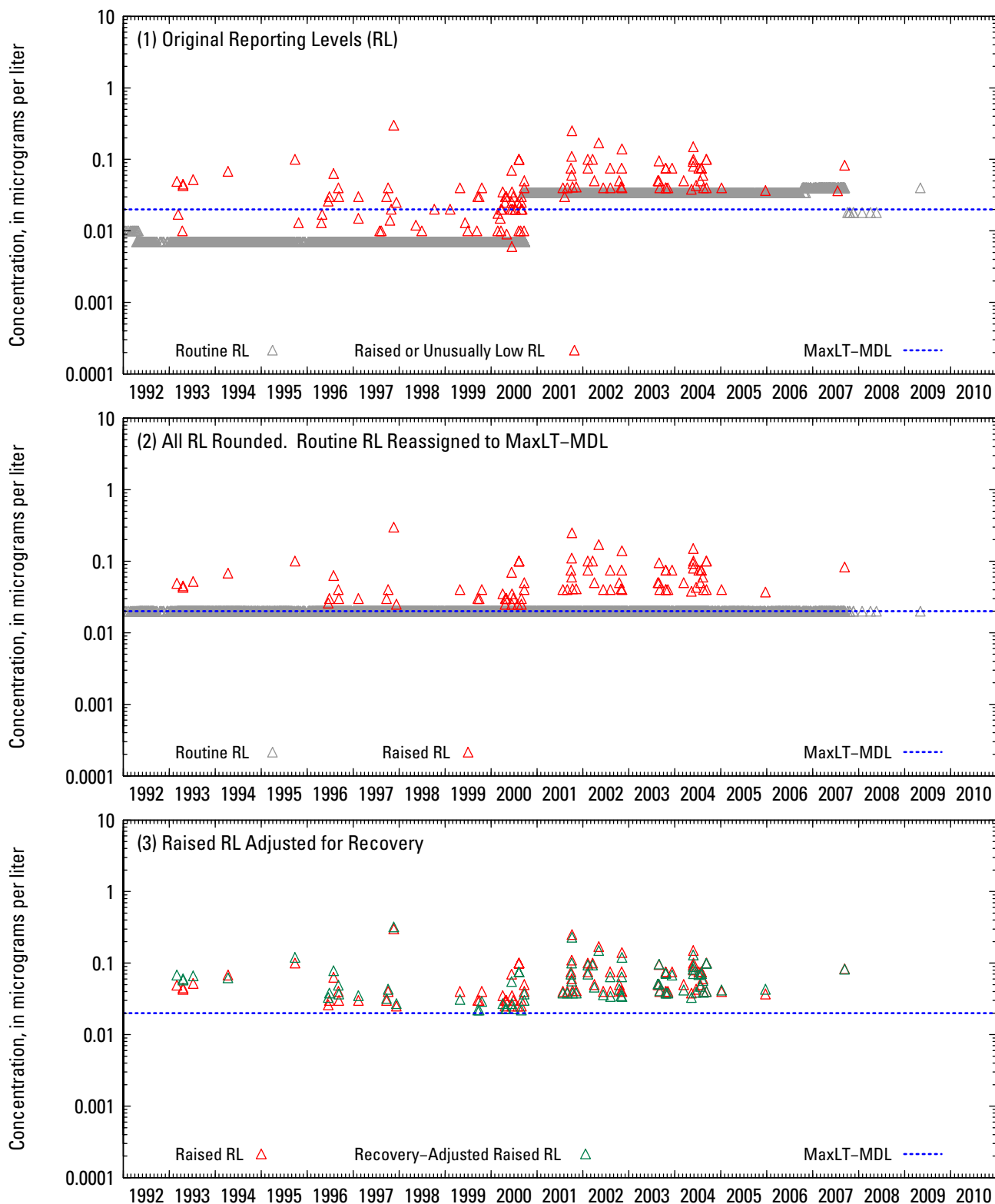
Figure 1–46. Time–series plots of nondetections of simazine for all sites in the trend dataset showing (1) original reporting levels; (2) rounded reporting levels and, for routine nondetections, reporting levels reassigned to the maximum value of the long–term method detection level (maxLT–MDL); and (3) raised reporting levels adjusted for temporal changes in recovery. Temporal changes in recovery are shown in panel 2 of the figures in appendix 2.

Figure 1–47. Time–series plots of nondetections of tebuthiuron for all sites in the trend dataset showing (1) original reporting levels; (2) rounded reporting levels and, for routine nondetections, reporting levels reassigned to the maximum value of the long–term method detection level (maxLT–MDL); and (3) raised reporting levels adjusted for temporal changes in recovery. Temporal changes in recovery are shown in panel 2 of the figures in appendix 2.
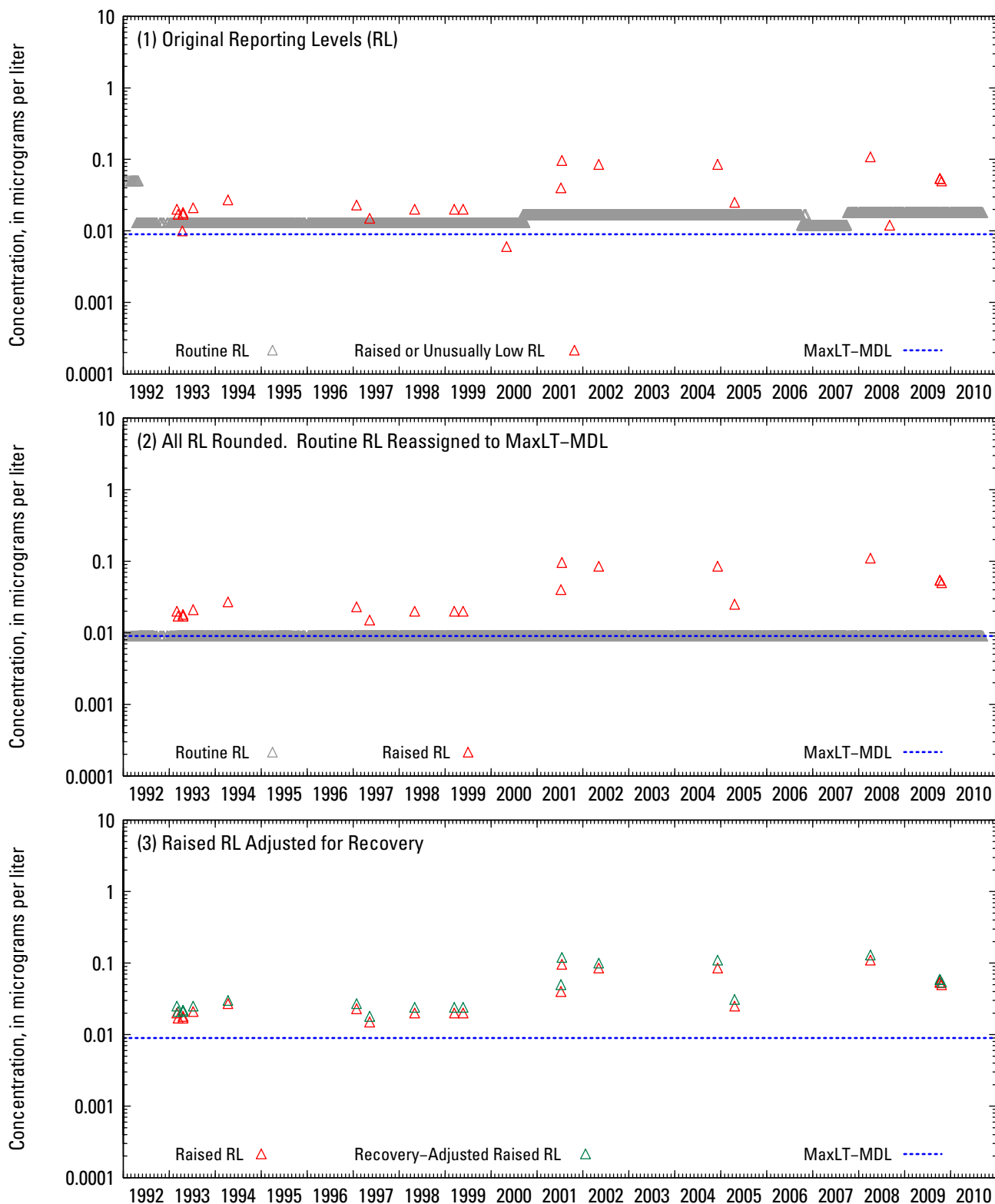
Figure 1–48. Time–series plots of nondetections of terbacil for all sites in the trend dataset showing (1) original reporting levels; (2) rounded reporting levels and, for routine nondetections, reporting levels reassigned to the maximum value of the long–term method detection level (maxLT–MDL); and (3) raised reporting levels adjusted for temporal changes in recovery. Temporal changes in recovery are shown in panel 2 of the figures in appendix 2.
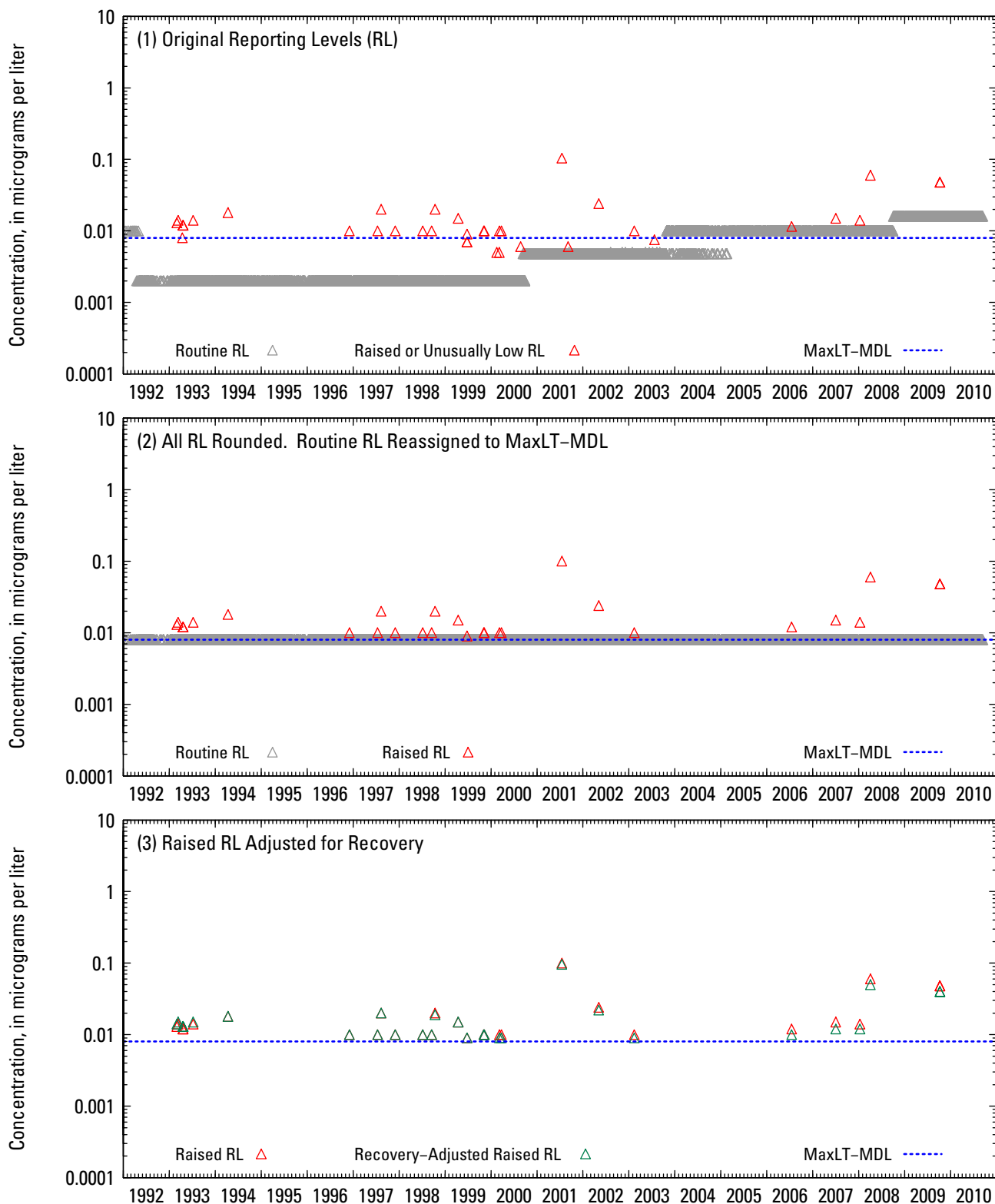
Figure 1–49. Time–series plots of nondetections of terbufos for all sites in the trend dataset showing (1) original reporting levels; (2) rounded reporting levels and, for routine nondetections, reporting levels reassigned to the maximum value of the long–term method detection level (maxLT–MDL); and (3) raised reporting levels adjusted for temporal changes in recovery. Temporal changes in recovery are shown in panel 2 of the figures in appendix 2.
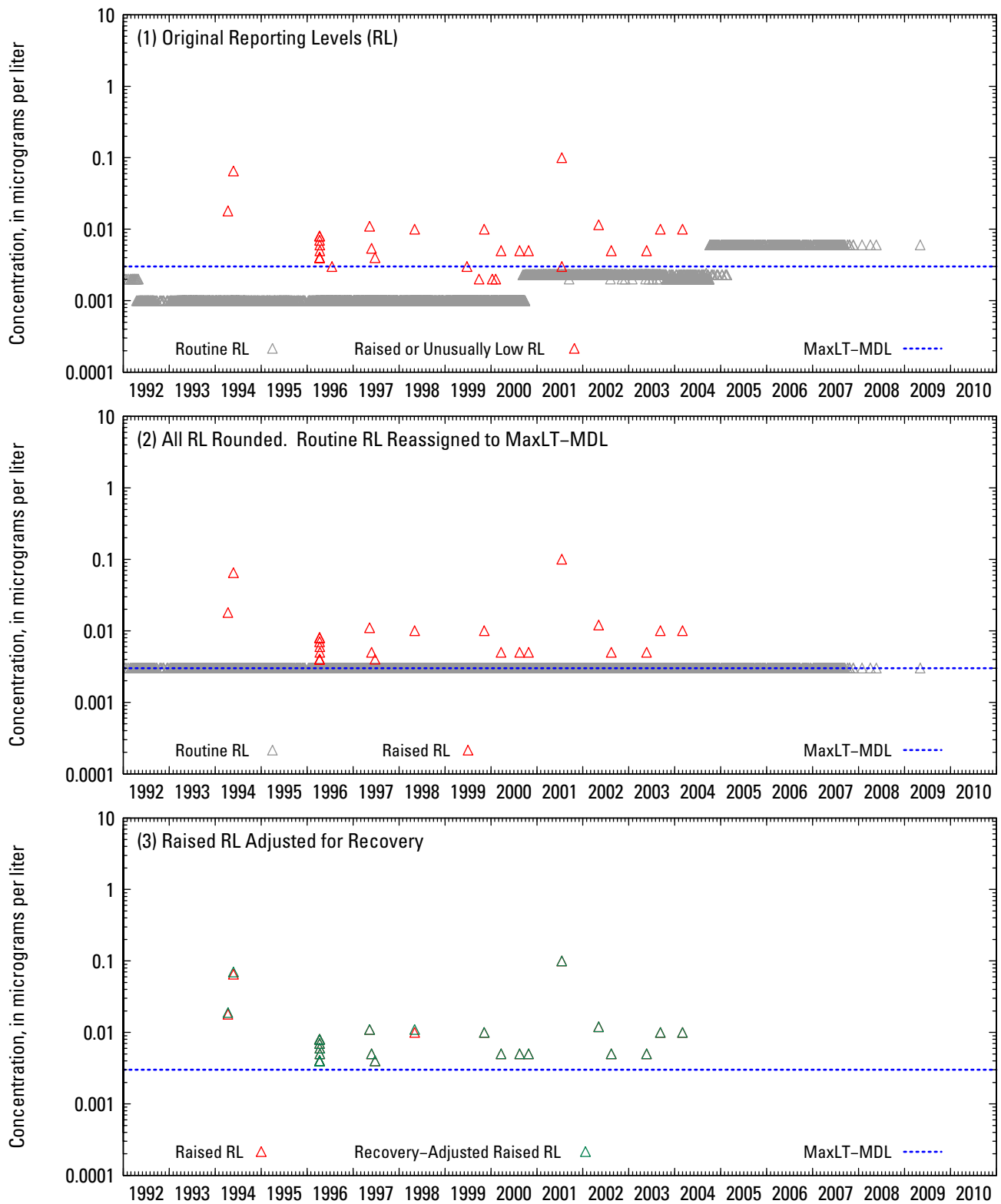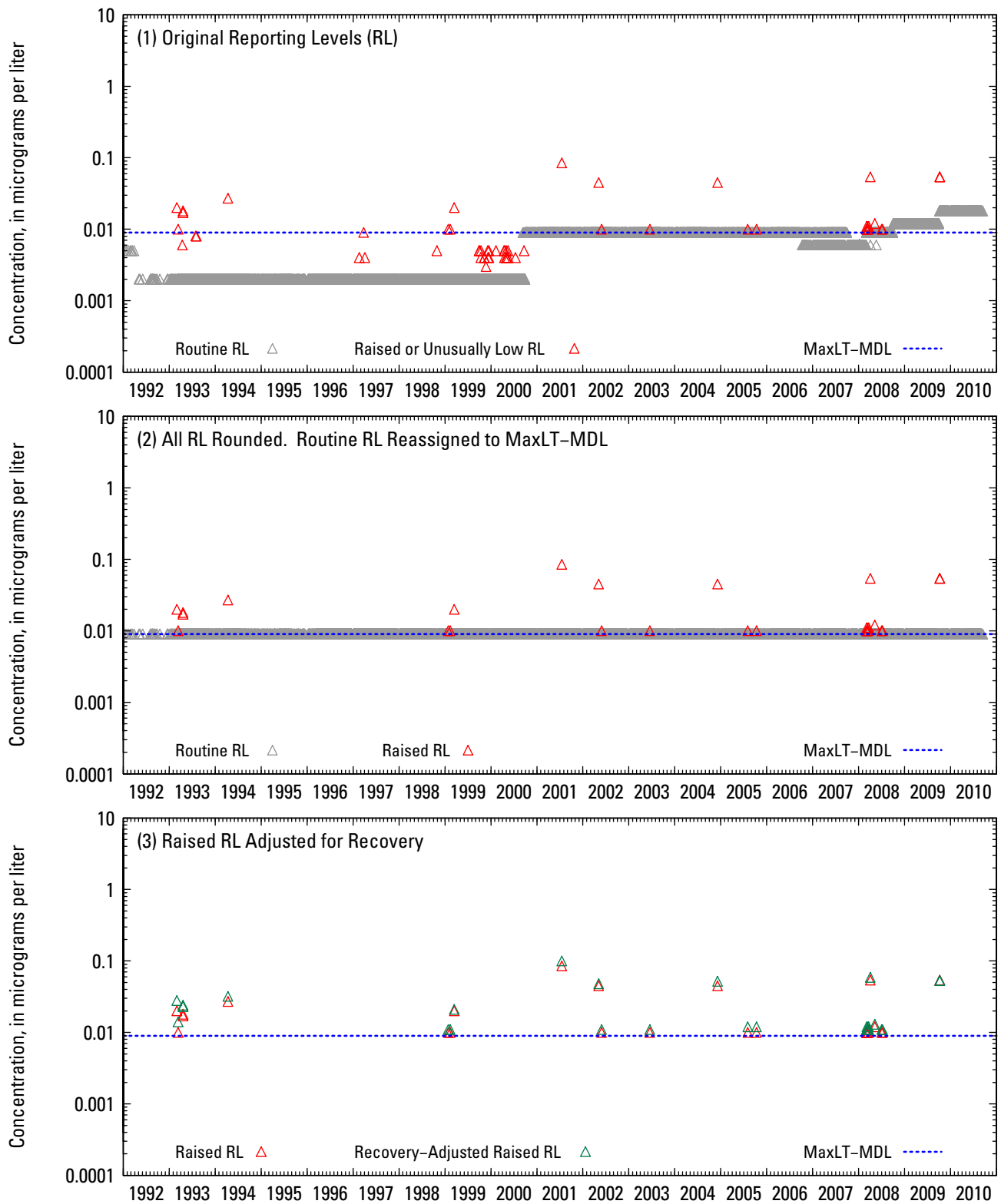
Figure 1–50. Time–series plots of nondetections of thiobencarb for all sites in the trend dataset showing (1) original reporting levels; (2) rounded reporting levels and, for routine nondetections, reporting levels reassigned to the maximum value of the long–term method detection level (maxLT–MDL); and (3) raised reporting levels adjusted for temporal changes in recovery. Temporal changes in recovery are shown in panel 2 of the figures in appendix 2.

Figure 1–51. Time–series plots of nondetections of triallate for all sites in the trend dataset showing (1) original reporting levels; (2) rounded reporting levels and, for routine nondetections, reporting levels reassigned to the maximum value of the long–term method detection level (maxLT–MDL); and (3) raised reporting levels adjusted for temporal changes in recovery. Temporal changes in recovery are shown in panel 2 of the figures in appendix 2.

Figure 1–52. Time–series plots of nondetections of trifluralin for all sites in the trend dataset showing (1) original reporting levels; (2) rounded reporting levels and, for routine nondetections, reporting levels reassigned to the maximum value of the long–term method detection level (maxLT–MDL); and (3) raised reporting levels adjusted for temporal changes in recovery. Temporal changes in recovery are shown in panel 2 of the figures in appendix 2.